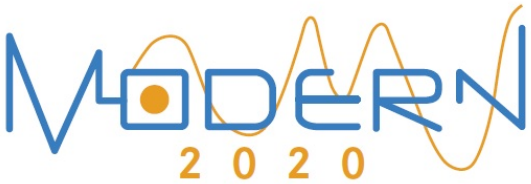

Contract Number: 622177

Deliverable D4.2:
Development of HA monitoring plan

Work Package 4

Project Acronym	Modern2020
Project Title	Development and Demonstration of Monitoring Strategies and Technologies
Start date of project	01/06/2015
Duration	48 Months
Lead Beneficiary	Andra
Contributor(s)	Radwan Farhoud, François Martinot, Johan Bertrand
Contractual Delivery Date	Month48 (May 2019)
Actual Delivery Date	31/05/2019
Reporting Period	3: 01/06/2018 – 31/05/2019
Version	Final

Project co-funded by the European Commission under the Euratom Research and Training Programme on Nuclear Energy within the Horizon 2020 Framework Programme		
Dissemination Level (for this draft of the report)		
PU	Public	X
PP	Restricted to other programme participants (including the Commission Services)	
RE	Restricted to a group specified by the partners of the Modern2020 project	
CO	Confidential, only for partners of the Modern2020 project	

History chart			
Status	Type of revision	Partner	Date
Milestones	Modern2020 Milestone 4.1	Andra	06.20.2017
Initial version	M2020_WP4_T4.2_V0	Andra	10.20.2018
Draft version	M2020_WP4_T4.2_V1 (send to GSL)	Andra	01.12.2019
2ndDraft version	M2020_WP4_T4.2_andra_final_report	Andra	30.04.2019
Version for review	M2020_WP4_T4.2_andra_final_report_V2	Andra	01.07. 2019
Final version	Modern2020_WP4_D4.2_HA_monitoring	Andra	19.08.2019

Reviewed by:

This report has been reviewed according to the Modern2020 Quality Plan and the Deliverables Review Procedure therein by Emilia HURET (Andra)

Approved by:

This report has been approved by:

- Jan Verstricht, Work Package 4 Leader, *19/08/2019*
- Johan Bertrand, the Modern2020 Project Co-ordinator (on behalf of the Modern2020 Project Executive Board), *19/08/2019*

List of accronym

HA:	Highly-active
HLW:	High-level waste
ILW:	Intermediate-level waste
LVDT:	linear variable differential transformer
MoDeRn:	Monitoring Developments for Safe Repository Operation and Staged Closure
Modern2020:	Development and Demonstration of Monitoring Strategies and Technologies for Geological Disposal – Horizon2020
MHM:	Meuse/Haute-Marne
OFS	optical fibre sensors
URL :	Underground Research Laboratory
VW	vibrating wire sensors
WP:	Work package

Table of Contents

List of figures

List of tables

1 Introduction

1.1 Background

The Development and Demonstration of Monitoring Strategies and Technologies for Geological Disposal (Modern2020) Project is a European Commission (EC) project jointly funded by the Euratom research and training programme 2014-2018 and European nuclear waste management organisations (WMOs). The Project is running over the period June 2015 to May 2019, and a total of 29 WMOs and research and consultancy organisations from 12 countries are participating.

The overall aim of the Modern2020 Project is to provide the means for developing and implementing an effective and efficient repository operational monitoring programme, taking into account requirements of specific national programmes. The Project is divided into six Work Packages (WPs):

- WP1: Coordination and project management.
- WP2: Monitoring programme design basis, monitoring strategies and decision-making.This WP aims to define the requirements on monitoring systems in terms of the parameters to be monitored in repository monitoring programmes with explicit links to the safety case and the wider scientific programme (see below).
- WP3: Research and development of relevant monitoring technologies, including wireless data transmission systems, new sensors, and geophysical methods. This WP will also assess the readiness levels of relevant technologies, and establish a common methodology for qualifying the elements of the monitoring system intended for repository use.
- WP4: Demonstration of monitoring implementation in repository-like conditions. The intended demonstrators, each addressing a range of monitoring-related objectives, are the Full-scale *in situ* System Test in Finland, the Highly-active (HA) Industrial Pilot Experiment in France, the Long-term Rock Buffer Monitoring (LTRBM) Experiment in France, and the Full-scale Emplacement (FE) Experiment in Switzerland. An assessment and synthesis of a number of other tests and demonstrators will also be undertaken, and this will include consideration of the reliability of monitoring results.
- WP5: Effectively engaging local citizen stakeholders in research and development (R&D) and research, development and demonstration (RD&D) on monitoring for geological disposal.
- WP6: Communication and dissemination, to include an international conference, a training school, and the Modern2020 Synthesis Report.

This report is the final report "Development of HA monitoring plan » of the Modern2020 Project. The document belongs to the second task of the WP4 dedicated to HA industrial pilot experiment, in Bure (France).

1.2 Objectives of this Report

This report addresses the following objectives of task 4.2:

- Evaluate a possible monitoring system dedicated to High Level – Long Lived radioactive (HL-LL) waste alveoli in Cigéo[1], according to the French concept;
- Identified a set of monitoring parameters to be tested into demonstrators;
- Describe qualification steps of sensing technologies, *in situ*, in full-scale demonstrators;

[1] Cigéo is the future French underground industrial plant for radioactive waste disposal

- Demonstrate the feasibility of monitoring alveoli in Cigéo project, according to the envisaged concept for the pilot phase[2].

  Provide (if any) the preliminary results and feedback on accomplished tests of monitoring system;

1.3 Purpose of the AHA Program to develop HLW cell design

In the Andra's URL, the AHA program unit dedicated to high-level waste alveoli has the following objectives:

- Realize HA0 cell with respect to the 2015 concept (i.e. using the filling material between metallic liner and host rock);
- Ensure the demonstrator meet the specifications (geometry, filling quality, etc.);
- Ensure that construction process is reliable (operating times, thrust forces applied, etc.);
- Evaluate the mechanical behaviour of the liner with filler material;
- Evaluate gaseous exchanges between the gallery and the HA cell;
- Check the feasibility of implementing measurement devices envisaged for monitoring.

The technology aim consists of checking that it is possible to construct HLW Cell based on the last concept design, which include the specific "filling material" between the metallic liner and the host rock.

The scientific issues in the "HLW cell" Programme Unit involve understanding the thermo-hydro-mechanical (THM) processes (and their characteristic time constants) at play on the sleeve's extrados (outer sleeve surface) and the physical and chemical state of the argillite and the sleeve steel at this extrados.

1.4 Rationale

The objective is to demonstrate Andra's ability to implement a monitoring system dedicated to HLW concept based on mature technology (≥TRL 7) (*see Modern2020 deliverable 3.1 for the TRL scale*), ie ready for implementation in the industrial pilot phase. This instrumentation must cover all environmental condition and technical requirements (*see Modern2020 deliverable D2.2*).

Experiments at the URL are conducted to validate concepts and methods to monitor the proposed parameters (*see screening methodology*). The monitoring program is conduct in way to:

- Propose measurement methods/technics aimed at checking the conformity of the structure with the specifications and requirements (acceptance testing) in addition to the data and surveys carried out during the construction of the structure (example: digging speed, deflection of the structure);
- Test implementation methods to the permanent instrumentation system for the monitoring of the parameters of interest with regard to long-term safety and reversibility needs;
- Validate the distribution (position, size, redundancy ...) of the instrumentation dedicated to a heavy instrumented HLW cell also called "witness cell" ;
- Define and consolidate the procedure for laying down the selected monitoring systems:
  - Reinforce the laying method for the selected sensors;
  - Arrange/organize the monitoring sections at the extrados of the liner;
  - Test different sensors configurations in function of the feedback
- Analyse redundant sensors
- To achieve a TRL 7 on the monitoring system component dedicated to HA cells.

[2] Short period of operation of Cigéo, about 5 years, to prove the feasibility and the safety of the envisaged concept

These tests would also make it possible to investigate the intrusiveness of the sensors

1.5 Specific objectives of the AHA1604 and ALC1605 Demonstrators

Inside the AHA program, the evaluation of the monitoring system is realized through a stepwise approach. Demonstrators named AHA1604, ALC1605 and AHA1605 are dedicated to evaluate progressively the monitoring system for HLW cell alveoli. Experiment is conducted from a light (AHA1604) to heavy instrumented (AHA1605) system.

These demonstrators are designed to:

- Demonstrate the ability to implement monitoring system in real condition with construction constraints;
- Qualify the monitoring design to provide Thermo-Mechanical and Chemical information, in representative conditions;
- Demonstrators are proof-of-concept about monitoring aspect;
- Demonstrate our ability to, continuously, monitor the integrity of structures in real-time during several decades;
- Qualify sensors in representative environment, which means increasing the maturity of some of them;
- Acquire and complete process knowledge like characteristic period of transitory phenomenon, or mechanical load monitoring, gas production, etc.

As a reminder, monitoring system must not affect the exploitation, neither in term of safety or in term of schedule or operational processes. Therefore, in order to be representative of Cigéo's operational conditions, Andra has chosen to install sensors on the extrados part of the metallic liner. This choice is compatible with cell being filled with waste packages, and it allows factice waste package to be introduced later, if decided.

Note : AHA1605 is not developed in this report due to late construction of this alveoli.. Objectives of the AHA1605 are described in the future work session

1.6 Report Structure

The report is set out as follows:

- Section 2 (Andra's monitoring approaches) describes the general approach of selecting monitoring parameters methodology and addressing requirements to each of them;
- Section 3 (Demonstrators concept in Andra's URL);
- Session 4 (AHA1604) describes the AHA1604 demonstrators;
- Session 5 (ALC1605) describes details about the ALC1605 experiments;
- Section 4 (References) presents a list of references cited in this report;
- Appendix : give technical details about material used during demonstrators.

2 HLW monitoring approach

2.1 The HLW concept

A distinction would be made between a disposal section for moderately exothermic HLW (HA0 in French) and disposal sections for highly exothermic HLW (HA1/HA2 in French). The design of these sections and their disposal cells differs in the moderate heat release from the waste, which allows higher disposal density and by the disposal schedule.

A pilot industrial zone will be built well before the operation phase and will contain a small number of moderately exothermic waste cells. This pilot industrial zone will allow a feedback. Additional progress with regard to knowledge and technical demonstrations can offer greater prospects of optimisation as part of the incremental development of Cigéo.

The design options and requirements defined for the HLW disposal cells and disposal sections in order to contribute to the accomplishment of the Cigéo safety functions are described below.

Each HLW disposal cell of Cigéo is blind with respect to the rest of the underground facility in order to limit water flows between the underground facility and the overlying formations via the surface-bottom connections after closure.

The small diameter structure group includes all HL waste disposal cells. These horizontal disposal cells will not be ventilated. A cylindrical envelope/sleeve of non-alloy steel provides mechanical stability. The inner diameters of the disposal cells will be approximately 70 cm. These disposal cells are illustrated in the following figure. This structural component responds to the requirements and allows the emplacement and potential retrieval of the waste disposal package: Its resistance to corrosion – at a minimum during the century scale operation phase – is ensured by its design and by placing the sleeve in a low-corrosion environment. The latter is achieved by the presence of a material between the clay rock and the sleeve contributing to a low corrosion speed and by preventing air exchange with the access galleries, thus providing for an anoxic environment.

It should be remembered that the limitation of the release of the radionuclides contained in the HLW waste is based in the first place on a low weathering rate of the vitrified waste. The weathering rate depends on the inherent characteristics of the glass and on the physicochemical environmental conditions in the HLW disposal cell, in particular the water properties (pH…) and the core temperature of the glass matrix when the water reaches the waste, which depends on the durability of the disposal overpack leak tightness. Andra is consequently designing the HLW disposal cell to support the durability of the disposal overpack initially and then, after loss of overpack leak tightness, the slow dissolution of the glass and the precipitation of most of the radionuclides.

The disposal overpack is protected by giving to the sleeve the highest possible mechanical durability, taking into account scientific uncertainties, technological limits and economic factors; this delays any contact between the sleeve and the disposal overpack during the operation phase. The overpack is also protected by avoiding a chemically-corrosive environment for both the overpack itself and the sleeve.

Like the disposal overpack, the sleeve is made of low-carbon unalloyed steel; this material withstands the mechanical stresses applied by the clay rock, and has a predictable long-term corrosion mode that avoids any risk of galvanic corrosion between sleeve and overpack.

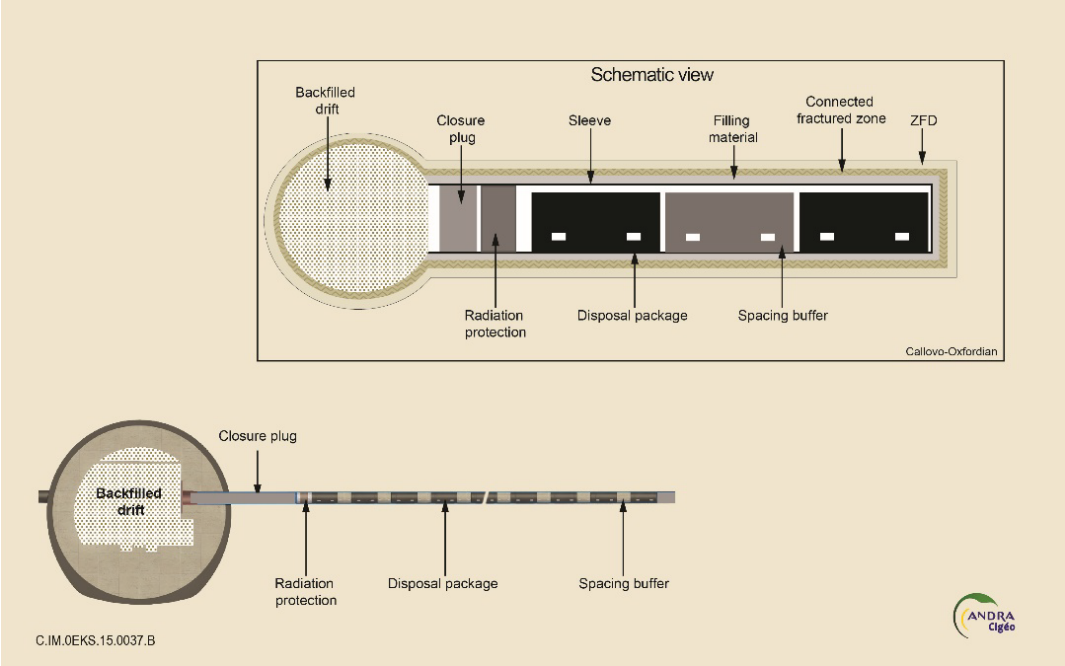

Figure 1 : Scheme of the HLW disposal cell design

Thermal processes

At the level of the disposal cell (internal and near field), the thermal head in near field is reached during the period of operation: on the basis of established design, the maximum temperatures are reached between about 5 to 10 years depending on the type of HLW disposal cell.

After 100 years (HA0) to a few hundred years (HA1 / HA2), the temperature in a disposal cell is broadly homogeneous: it is around 35 °C in a moderately exothermic disposal cell, and from 50 to 80 °C in a highly exothermic disposal cell and in near field.

Hydraulic processes

In the post closure short term, the exothermicity of HLW results in a temperature increase which implies, particularly in clay host rock at the centre distance between cells, an increase in pressure of the pore water during its thermal expansion (up to 10-12 MPa). The favourable properties of the clay host rock are preserved.

In parallel, but also in the longer term, conditions become anoxic and corrosion rates are then low. This phenomenon produces hydrogen, which prevents total resaturation of the disposal cell during several tens of thousands of years at least.

Mechanical processes

In situ mechanical loading of the sleeve was investigated on reduced and full scale HLW cell demonstrators drilled in the Meuse/Haute-Marne URL. All the measurements led to an anisotropic loading whether with or without cement grout in the annular space between the sleeve and the rock. This behaviour is govern by the anisotropic extent of the excavation induced fractures network around the cell. The resulting radial bending of the sleeve leads to its ovalization, which can reach 1% of the diameter after 5 years. Convergence rate is decreasing with time and an extrapolation over 100 years leads to a maximal diameter variation of about 1.5%. During this period, overpacks are only subjected to a non damaging external hydrostatic pressure.

Chemical processes

To control the functioning of a HLW disposal cell, the most chemical important process is the corrosion of metallic components such as the sleeve and the overpack between 100 and 1000 years and the glass dissolution after 1000 years.

2.2 Monitoring parameters identification

The method chosen by Andra, to define its needs in terms of processes and parameters to be monitored, has been analysed for each component of the repository. This method take into consideration

- Safety functions;
- Phenomenological processes in link with safety functions;
- Quantification of phenomenological processes in link with safety functions;
- Selected indicators/parameters of phenomenological processes in link with safety functions;
- Monitoring apparatus/ technology;
- Data management.

This method for selecting the monitoring parameters differs slightly from that proposed under Modern2020, in particular as regards the starting point and the steps dedicated to the processes.

Detailed can be founded in the Modern2020 deliverable 2.2 of the WP2. The results of the monitoring parameters selection can be found in the following table (Table 3).

Table 1 Parameters identified in the Cigéo test case

Parameter	Component	Reasoning for monitoring parameter	Technology option for monitoring as results of the present test case
Temperature	Disposal cell / near-field rock	Relevant to post-closure safety and retrievability (information about possible rock deformation).	Monitored directly in some cells using Pt probe and/or optical fibre sensors.
Porewater pressure	Near-field rock	Relevant to post-closure safety (information about thermal induced pressurization of the clay host rock)	Monitored directly using vibrating wire or optical fiber piezometers.
Confining pressure	Total pressure on cell sleeve	Relevant to demonstrating retrievability of the disposal packages (information about the mechanical load acting on the cell sleeve)	Monitored directly in some cells, using optical fiber sensors.
Displacement	Cell sleeve	Relevant to demonstrating retrievability of the disposal packages (information about the deformation of the sleeve)	Monitored directly in some cells using optical fiber sensors and 3D scan.
Strain	Cell sleeve	Relevant to demonstrating retrievability of the disposal packages (information about the deformation of the sleeve)	Monitored directly in some cells, using optical fibre sensors.
Hydrogen concentration	Cell atmosphere	Provides information about the cell atmosphere as data for the retrievability of the disposal packages and about the environment conditions of corrosion	Monitored directly in some cells using LiDAR and/or thermal gas conductivity and/or gas density and viscosity measurements.

Parameter	Component	Reasoning for monitoring parameter	Technology option for monitoring as results of the present test case
Oxygen concentration	Cell atmosphere	Provides information about the cell atmosphere, as data for the retrievability of the disposal packages and about the environment conditions of corrosion.	Monitored in some cells using LiDAR.
Relative humidity	Cell atmosphere	Provides information about the corrosion of sleeve and overpack, which is relevant to demonstrating retrievability of the disposal packages and to post-closure safety (environment conditions).	Monitored in some cells using capacitive sensor (based on an electrical capacitor).
Porewater pH	Near-field rock	Relevant to post-closure safety (information about the neutralisation of the filling material)	Monitored in some cells (based on pH meter)
Thickness	Cell sleeve	Relevant to demonstrating retrievability of the disposal packages.	Monitored in some cells using corrosion coupons.
	Overpack	Relevant to post-closure safety.	Monitored in some cells using corrosion coupons.
Corrosion rate	Cell sleeve	Relevant to demonstrating retrievability of the disposal packages.	Monitored indirectly in some cells using electrical resistance probes and mass loss of coupons.
	Overpack	Relevant to post-closure safety.	Monitored in some cells using electrical resistance probes and mass loss of coupons.

2.3 Sensor qualification procedure

For all developments, Andra has specified a multi-stage qualification procedure, to ensure robustness and thorough metrological understanding of the developed measurement chains, and aims at defining and implementing corresponding reference standards. To illustrate this recommended approach, a succinct description of the qualification process that Andra has put in place[3] is provided. It entails testing and qualifying the complete measurement chain, by progressive steps, knowing, to be able to anticipate them, the failure rates and mastering the possible long term drifts. Four steps were identified.

The overall process is inspired from the qualification guide for non-destructive methods[4]. Global test sequence includes four stages.

- Stage one consists in acquiring in-depth knowledge of the sensing technology, engineering solutions, practical implementation constraints. It aims at selecting the technologies best suited to the specific requirements of monitoring the geological

[3] Developing the tools for geologic repository monitoring - Andra's monitoring R&D program, S Buschaert, S Lesoille, J Bertrand, S Mayer, P Landais WM2012 Conference, February 26-March 1, 2012, Phoenix, Arizona, USA

[4] Qualification guide FD CEN/TR 14748 "Non-destructive testing – Methodology for qualification of non-destructive tests" 2005

repositories for long-lived nuclear wastes. When commercially-available sensing chain performances do not fulfil requirements, Andra initiates research programs;

- Stage two consists in carrying out laboratory tests, under fully supervised and/or controlled environmental conditions, to qualify the sensitive component and assess the complete measurement chain performances. Sensors are tested in air, and embedded in host material of interest;
- Stage three consists in outdoor tests, to evaluated field implementation influence. At this stage, the sensing chain is preserved from hazardous conditions, extreme temperature or gamma rays. Unexpected influence parameters might thus be revealed.
- Fourth stage involves hardening in view of the application environmental conditions. In the envisioned French geological repository, temperature would range from 25°C to 90°C. Gamma radiation rates reach Gy/h, total dose 10^7Gy. Hydrogen release is also expected; its maximum levels could approach 100% hydrogen content in the atmosphere.

More details can be found in the Modern2020 deliverable D3.6.

2.4 Background on optical fiber sensors

For underground repositories, optical fiber sensors, sensor multiplexing ability is very attractive. Distributed technologies, i.e. continuous measurements along the optical fiber without requiring a preliminary definition of the exact measurement site, generates extremely promising prospects in the field of instrumentation. Instruments providing strain and temperature distributed measurements are now commercially available. They rely on scattering phenomena into silica cores of fibers, combined with localization processes (such as pulse-echo).

AHA program ambition to progress on the capability to implement suitable optical fiber sensors. Some basic consideration are reminding in the following paragraph in order to better understand some experimental issues.

2.4.1 Principles: scattering phenomenon and localization processes

The term *distributed sensor* designates the case in which the optical fibre itself becomes a sensor. It is thus no longer necessary to implement anticipated sensor positions since measurements are being performed all along the optical fibre plugged up to the reading device (as well as within the extension cables!). For distributed OFS, the commercial optical fibre is placed directly inside its mechanical protective coating, which would suggest a more robust instrumentation. It associates principles based on optical scattering, sensitive to strain and temperature variations as described below in “Principles for temperature and strain sensing,” with localization processes described below in “Principles for localization”.

Principles for temperature and strain sensing

As shown in Figure 2 the light backscattered by an optical fibre segment without any defects or abnormal characteristics is spectrally decomposed into three distinct peaks corresponding to three outstanding phenomena.

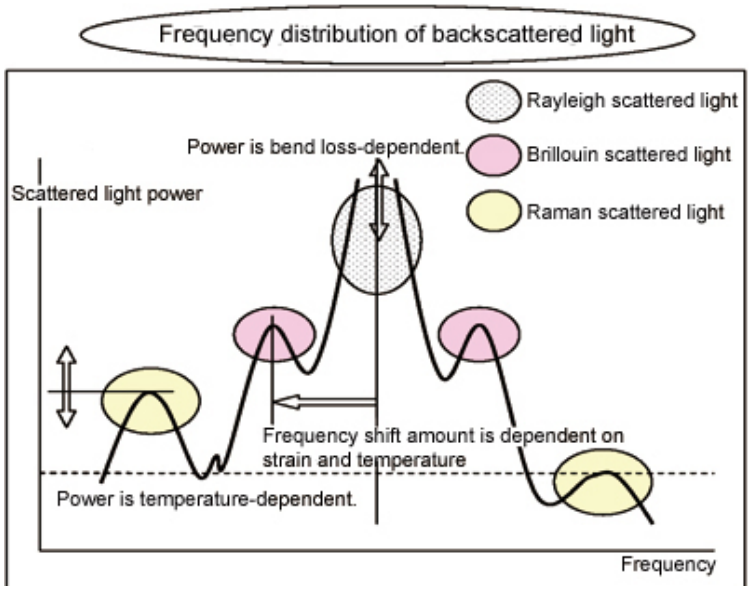

Figure 2: Spectrum of backscattered light inside an optical fibre

2.4.2 Rayleigh scattering

The first scattered light relates to Rayleigh scattering. The electromagnetic wave propagating in the fibre core interacts with the scattering centers, silica impurities and enhancing additives with dimensions well below the wavelength. By measuring intensity variations in the backscattered signal at the same wavelength as the injected wave, local optical fibre modifications may be detected: an abrupt return peak is interpreted as a mirror reflection (connector or damage on the fibre), and a sudden drop in intensity corresponds for example to shear loss., however, light intensity variations cannot be directly correlated with deformations of the medium where the optical fibre has been embedded.

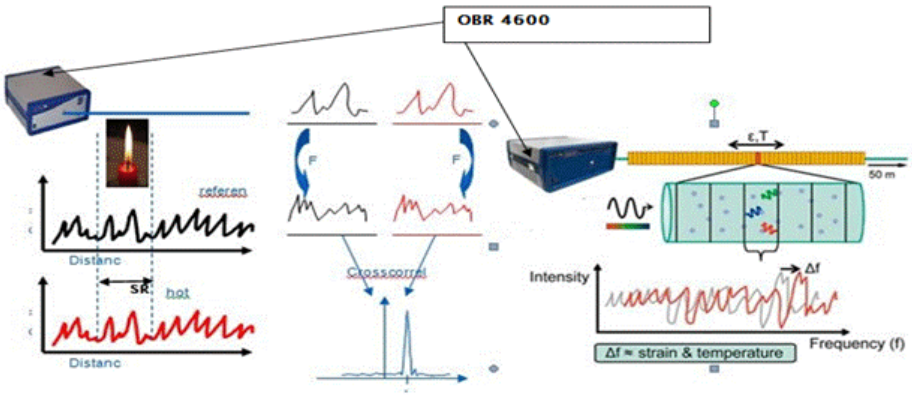

Figure 3: OBR measurement principle

The estimation principle of strain or temperature variation of the optical fibre between two states is shown in Figure 4. The technique is to perform two OFDR such measures, a reference (in black) and second (in red) with the fibre in a modified state-owned (change in temperature or strain). The comparison of the signals is performed in the frequency domain, by selecting a particular area of the fibre and applying a Fourier transform to the data of the selected area in the two states. $\Delta\nu_R$ the frequency shift is determined by cross-correlation. It corresponds to changes in the backscatter spectrum in this area

The American firm Luna Technologies has been marketing since spring 2006 an optoelectronic device that enables measuring optical fibre strain (at a constant temperature, or the opposite, that is to say temperature at a constant strain) over 150 m with a millimeter-sized spatial

resolution and a level of precision equal to a few microstrains. This performance has been obtained by OFDR, in association with an advanced correlation method between the ongoing measurement and a reference state; the spectral lags of the Rayleigh backscattering peak can thus be analyzed

2.4.3 Raman Effect

The Raman Effect is an interaction between light and the corresponding coupling matter between a photon and the thermal vibration of silica molecules. As such, this phenomenon is highly dependent on temperature. More precisely, the anti-Stokes intensity evolution (low frequency component) must be augmented with a reference measurement since optical fibre losses vary with time (increase with fibre aging, connector dirt or optical fibre curvatures etc.). A solution commercially implemented is to analyse the ratio between the Anti-Stokes and Stokes (high frequency component) absorption line intensities (I_{RAS} and I_{RS}). To perform distributed temperature measurement, Raman scattering is the most advanced technology.

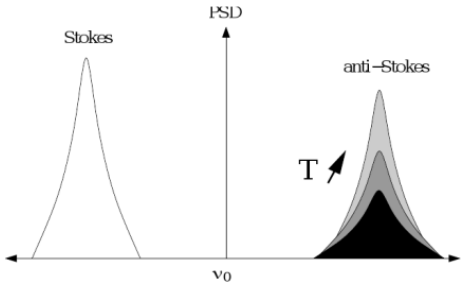

Figure 4: Raman scattering sensitivity to temperature ("PSD" stands for power spectral density)

More equipment about Raman scattering originates from laser light photon interaction with thermal vibration of silica molecules (thermal phonons). More precisely, as sketched in Figure 5, the anti-Stokes absorption mainly depends on temperature. As a consequence, Raman distributed sensing systems may use Optical Time Domain Reflectometry (OTDR) pulsed technique to perform distributed intensity measurement of the anti-Stokes backscattered light. However, the anti-Stokes intensity evolution must be augmented with a reference measurement since optical fibre losses vary with time (increase with fibre aging, connector dirt or optical fibre curvatures etc.). A number of commercially available distributed temperature sensing devices automatically compensate for this loss by analysing the ratio between the Anti-Stokes and Stokes absorption line intensities.

Instrumentation set-up

In order to probe a previously installed fibre optic line, the instrumentation is typically set-up as shown in Figure 6. The instrument box contains a pulsed laser source, capable of launching multiple laser light pulses whose duration may be 10 ns or less. These laser pulses are directed to the fibre line by means of a directional coupler. The fibre optic line then passes through an oven or bath of a known reference temperature.

First of all, the laser source emits a narrow light pulse which passes the optical coupler and enters into the optical fibre. When travelling through the fibre, the Raman Effect occurs along the fibre, and the backscattered light is transmitted back along the fibre. Then the light goes through the optical filter and is divided into two components: Stokes light and Anti-Stokes light. Then the components go further into the optical sensor, where they turn into electrical signals representing the light intensity. After the A/D converter, the data is sampled into a computer for signal processing and temperature decoding

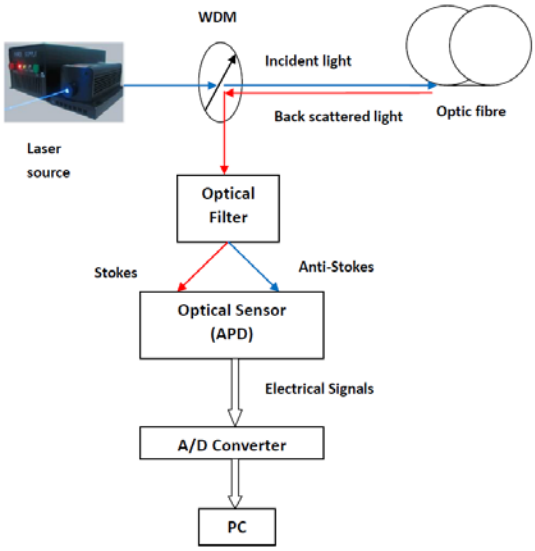

Figure 5: Instrumentation for initiating and analyzing the backscattered light.

2.4.4 Brillouin

The interaction between an electromagnetic wave and matter can generate variations in the molecular structure of the material. Classically, the incident light wave generates acoustic waves through the electrostriction effect (electrostriction is the tendency of materials to become compressed in the presence of an electric field) and induces a periodic modulation of the refractive index of material that provokes a light-backscattering like a Bragg grating. This scattered light is down-shifted in frequency due to the Doppler shift associated with the grating moving at the acoustic velocity. From the point of view of quantum physics, when the intensity of light can modify locally the density of the solid, a scattering process can appear. In this process the material absorbs part of the energy from the electromagnetic wave. This energy is used for generating a periodic structure, while the remaining energy is reemitted as a wave of lower frequency, provided that conditions of resonance between the light wave and the phonon are met. The scattering associated to this process was named as "Brillouin scattering" after Leon Brillouin did for the first time the theoretical description in 1910.

Spontaneous scattering of light is mostly caused by thermal excitation of the medium, and it is proportional to the incident light intensity. On the other hand, the scattering process becomes stimulated if fluctuations in the medium are stimulated by the presence of another electromagnetic wave that reinforces the spontaneous scattering. The scattering process is in the stimulated regime provided that the intensity of the input light has a value above a level known as the threshold, which is lower than the threshold of the spontaneous regime. The stimulated scattering process is readily observed when the light intensity reaches a range between 106 and 109 Wcm^{-2} [25] and is capable of modifying the optical properties of the material medium.

Stimulated Brillouin Scattering (SBS) can be achieved by using two optical light waves. In addition to the optical pulse, usually called the pump, a continuous wave (CW), the so-called probe signal, is used to probe the Brillouin frequency profile of the fibre [26]. A stimulation of the Brillouin scattering process occurs when the frequency difference of the pulse and the CW signal corresponds to the Brillouin shift and provided that both optical signals are counter-propagating in the fibre. The interaction leads to a larger scattering efficiency, resulting in an energy transfer from the pulse to the probe signal and an amplification of the probe signal.

Brillouin scattering is strongly dependent on thermodynamical variables. The dielectric constant varies according to the pressure wave that is generated and which travels along the medium. Then, the Brillouin shift frequency is a function of the acoustic phonon, as well as the medium structure and its constituents. The material structure is clearly perturbed by changes on environmental temperature or by strong alterations on its density distribution; such is the case

when a longitudinal force or a stress is applied. Those transversal or longitudinal forces relay on a shrinking or an enlargement of the original size of the material.

The Brillouin frequency shift has a linear dependence (for values of strain and temperature within its tolerance ranges) on the applied strain and the temperature variation (at a reference temperature) that can be written as

$$\upsilon_B (T, \varepsilon) = C_\varepsilon.\Delta_\varepsilon + C_T.\Delta_T + \upsilon_B (T_0, \varepsilon_0)$$

Where is the strain coefficient (MHz/), is the temperature coefficient (MHz/°C) and reference strain. These values are mostly determined by the fibre composition, pump wavelength, fibre coatings, and jackets.

Brillouin scattering was proposed for the first time to measure temperature in 1989 [30], and, currently, it is widely used for distributed temperature and strain sensing because the Stokes side-lobe is temperature and strain dependent. One reason of this success is that Brillouin effect can be used in long transducers (hundreds of kilometers) made of standard singlemode telecommunication optical fibres, since the Brillouin frequency shift is about 10-11 GHz at 1550 nm. An example of this dependence for a standard single mode fibre (SMF) is shown in Figure 7.

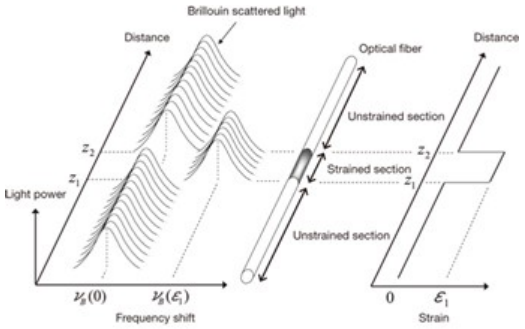

Figure 6: Example of distributed strain measurement in the case of Brillouin scattering

3 Setting up HA demonstrators in Andra's URL

3.1 Underground laboratory facility

3.1.1 Host rock description

Geologically, the Meuse / Haute-Marne site (French host rock) corresponds to a part of the eastern region of the Paris Basin. In this region, the Paris Basin is composed of alternating sedimentary predominantly argillaceous and limestone layers, deposited in a stable marine environment during the Jurassic (165 – 135 Ma). These layers have a simple and regular geometric structure, and slope slightly toward the northwest (1 degree) in accordance with the general structure of the Paris Basin (bowl-shaped structure centered in the Paris area). Within the sedimentary sequence, the Callovo-Oxfordian layer has been selected for hosting a deep geologic repository.

The structural framework is stable, with natural mechanical stresses oriented in the same direction for the past 20 million years. From a seismotectonic perspective, the Paris Basin is a stable zone with very low seismicity, remote from active zones such as the "Fossé Rhénan" toward the east, the Alps (southeast), the Massif Central (south) and the Massif Armoricain (west). There is no detectable neo-tectonic activity or significant local seismic activity in the Meuse / Haute-Marne region, as indicated by the national seismic monitoring network and the local monitoring network implemented by Andra.

The Callovo-Oxfordian formation is a sedimentary clay-rich formation. It mainly consists of clay minerals (e.g., mainly illite and illite/smectite interlayered phases), representing up to 60% of the total rock mass, silts (fine quartz) and carbonates.

A large zone of study for the characterization of the geological medium was defined in 2005 by Andra, within which the Callovo-Oxfordian layer has physical and chemical properties similar to those observed at the URL. This zone is called the Transposition Zone (ZT). Based on the complementary studies developed on the transposition zone and in the URL, Andra proposed in 2009 a 30 km² zone of interest for detailed survey (ZIRA) to obtain more precise information for the implementation of a future repository. In the ZIRA area, the depth to the top of the Callovo-Oxfordian across this zone varies from 340 m to over 530 m, and the thickness of the layer itself varies from 140 m to 160 m.

The absence of fractures in the investigated zone, the overall very low permeability, the absence of preferential flow paths, the favourable geochemistry (reducing environment, low solubility of radionuclides) are important elements in the safety case that allow the evaluation of transfer through the host formation as diffusion-dominated transport for those radionuclides that are in solution and not strongly sorbed. Any activities (e.g. excavation) or evolutions (e.g. desaturation-resaturation, heating, chemical interactions) that may have an impact on this must be well understood and taken into account.

In addition, these water transport properties of the host rock (diffusion-controlled flux rates) limit near field desaturation during operation in ventilated access tunnels and disposal drifts. They also limit resaturation after drifts and tunnels have been closed. This also has implications on the mechanical properties. In addition, due to the very low permeability of the host formation, the only expected interaction with overlying formations is related to access shafts and access ramps.

Anisotropic stress state of the claystone wasdetermined. The major principal stress component is horizontal and oriented in the range N155E + 10". The ratio σH/σh and σV/σhis about 1.3 and 1.0 respectively at the main level of the URL This anisotropic stress influences the extension of the fractured zone, induced by digging process around the structures. For structures oriented to the minor horizontal stress (N65 ° E), the extension of the damaged zone develops preferentially along the vertical, whereas in the direction of the major horizontal stress (N155 ° E), the extension develop preferentially following the horizontal.

.

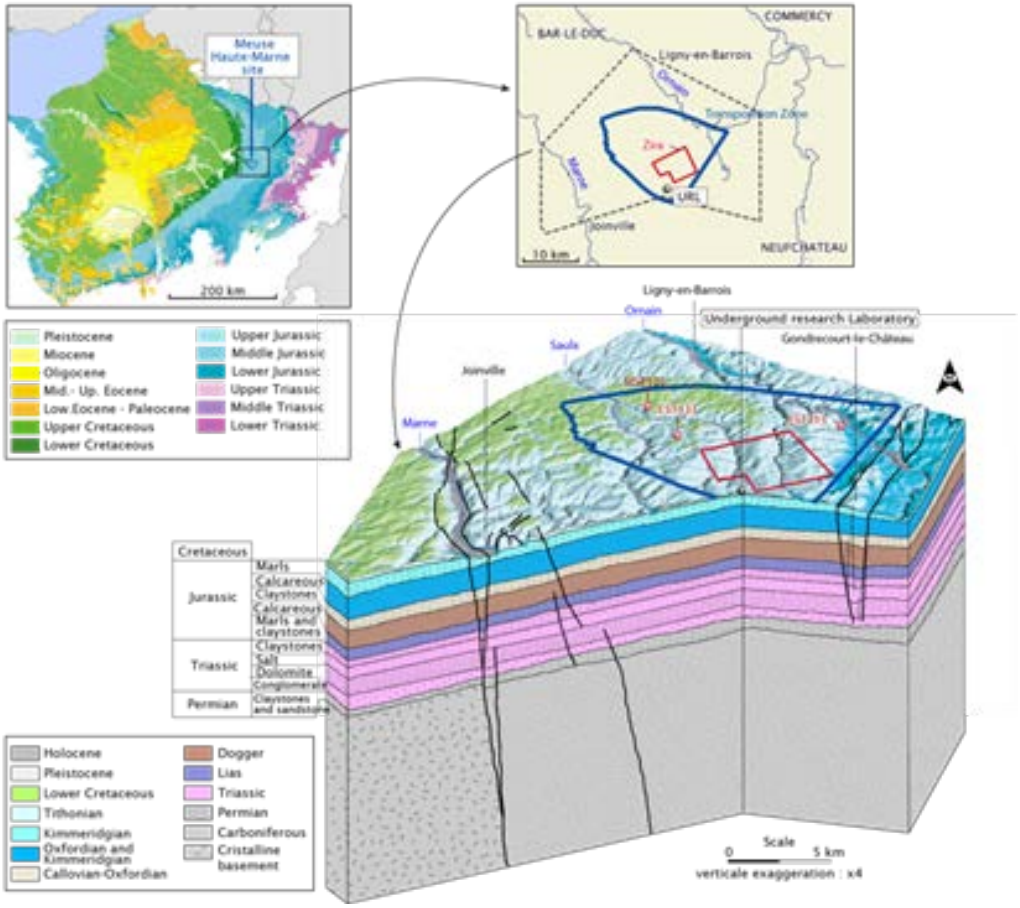

Figure 7: 3D geological block diagram of Meuse / Haute-Marne site

3.1.2 URL layout

Figure 8 shows the actual and forecast network of drifts and shafts at the MHM URL. Two shafts provide access to two levels of drifts at depths of 445 m and 490 m. All experiments relative to the THM behaviour study and HLW-LL cells have been performed at the main level of the URL in the clay unit where the disposal cells will be implemented in the disposal facility

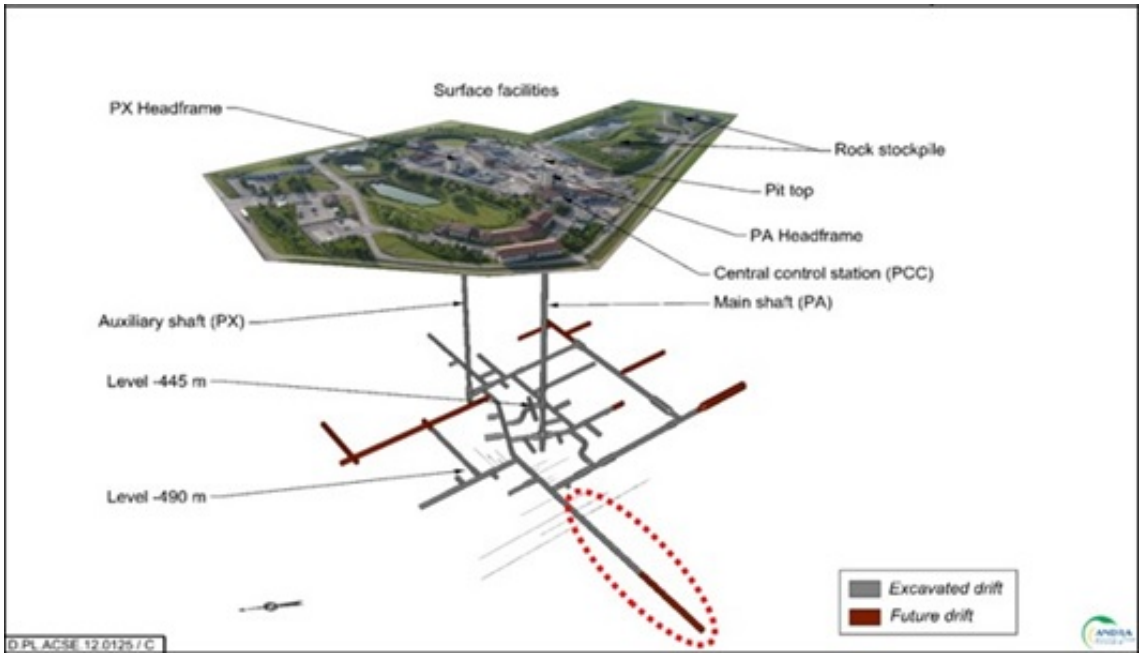

Figure 8: overview of Meuse/Haute Marne Centre (CMHM), underground laboratory and surface facilities with ellipse in dated red line of gallery GAN were demonstrators of HLW alveoli are planned.

3.2 General construction principle for HLW demonstrators

The demonstrator is designed to be as similar as possible to the reference concept in Cigéo for HLW cells. This similarity concerns construction, materials and monitoring system. In Andra's URL, cells should be adapted to limitations in the laboratory. As an example, galleries diamater in the URL, where it's planned to excavate HL-LL cells, is 4.5m.

The following table illustrates mean elements of the cell, in Cigéo and what was decided to test in Andra's URL in the framework of this demonstrator

Table 2 Synthesis of reference concept and demonstrator features

Cell's component	Cigéo's reference concept for HL-LL radioactive waste cells	Demonstrator's chosen options
Excavation technic	**Cell totally excavated and then introducing of pipes in one time**	
Excavation diameter (mm)	800 – 920	**920**
Pipes' steel reference	API 5L X65 MS PSL 2	API 5L X65 MS PSL 2
Excavation orientation	σH	σH
Tilt	Cell axis, up : 2 % +/- 1 % in each point of the cell (back-bent forbidden)	
Azimuth	Cell's axe oriented : N155° or N335° (according to σH) +/- 1 %	
Pipes dimensions	Ø outside 660 mm (26'') or 762 mm (30'') Thickness: 25.4 mm (1'')	Ø outside 762 mm (30'') Thickness: 25.4 mm (1'')
Length	80-150 m	80 m
Cell's bottom	Closed	First tube equipped with cement injection system
Insert	Mobile insert with concrete station bloc for waste package transport's engine	Note envisaged
Bride	Provisory radioactive tight closer	Note envisaged
Pipes connection's type	Clipped	Clipped with cement material proof joint

Surrounding filled materials	Yes	Yes
Water collecting device	Integrated to insert	Note envisaged
Cell's closer device	Radiological closer device + bride	To be determined during conception phase

3.2.1 Cell excavation/emplacement of the casing

In terms of excavation works, a specifical drilling machine was designed, fabricated and installed in situ and brought into operation (Figure 13). The drill head can be adapted to excavate diameters of 70–75 cm. It also allows the drilling machine to be withdrawn once excavation is completed, by rotating in the opposite direction as that used for excavation. Drilling is carried out with air. The machine is laser-guided, providing good control of the micro-tunnel trajectory and the drilling parameters (thrust applied on the cutting wheel, thrust applied on the casing, cutting wheel torque, rotating speed, rate of penetration) are recorded. The casing is made of steel tubes 2 m long, 70 cm in outer diameter and 2 cm thick, which can be welded or interlocked with each other as the excavation advances (see Figure 14)

Figure 9: micro-tunnel machine

Figure 10: handling metallic tube after the exacvation and before pushing them in the hole

The Figure 15 shows the main steps for the construction of the HLW alveoli in Andra's URL.

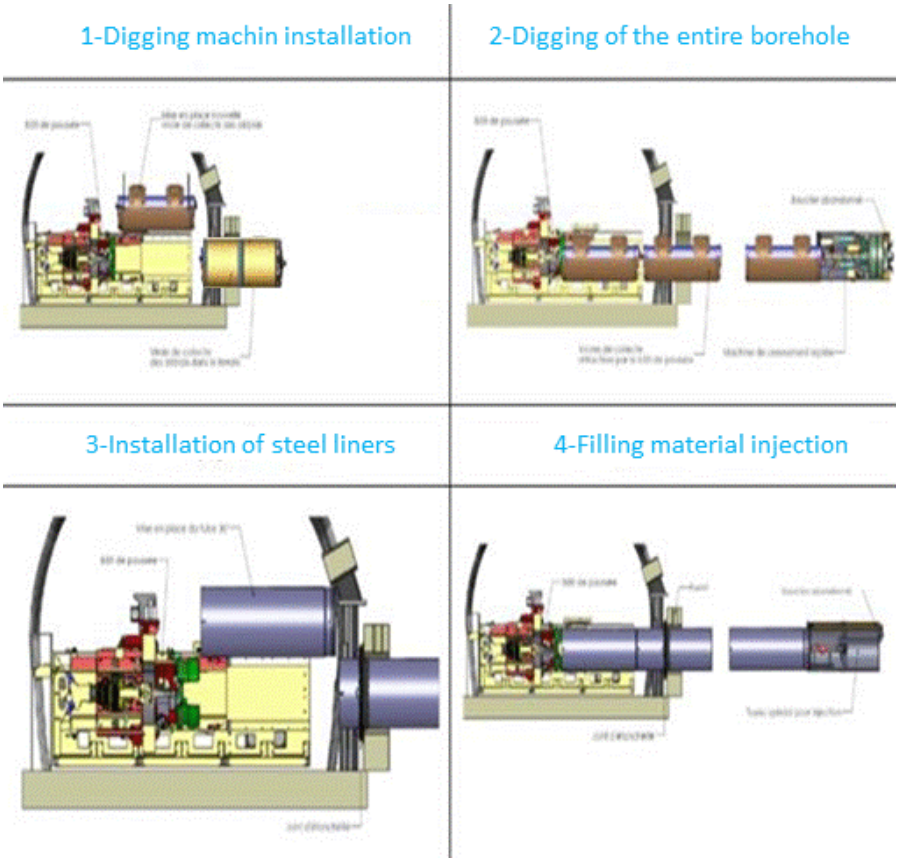

Figure 11: Sketch for the different construction step process in Andra's URL.

3.2.2 Filling material

The annular gap between the sleeve and the clay rock is filled with a material that imposes corrosion-limiting environmental conditions (cement-based grout). The injection of the material between the casing and the host rock is carried out by the inside of the casing, from the gallery via a pipe leaded to its bottom. Figure 8 presents the injection system in the first tube in the bottom of the casing. This system injects grouting material into the surrounding area between rock and casing (liner).

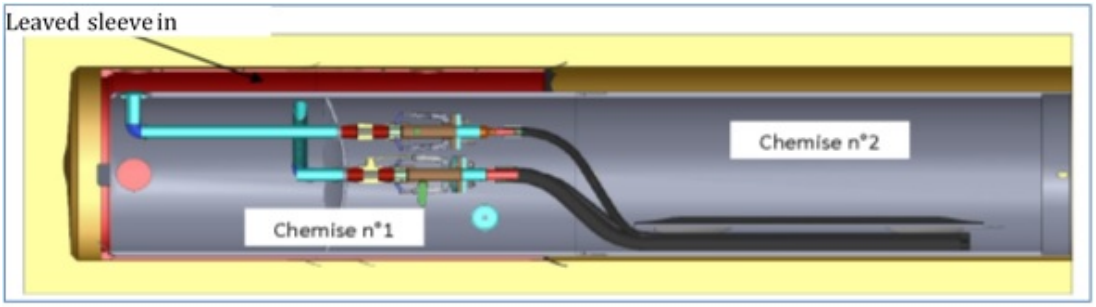

Figure 12: Injection system in the bottom of the casing of AHA1604

An annular sealing system equipped with a vent and injection piping are installed in the gallery. The maximum injection pressure is set to 10 bars. The control of the correct filling of the bottom of the alveolus is made by 2 vents (one outlet on the upper surface of the casing and one at the top of the volume collecting the residual rock debris). Ferrules collect breakouts at the end of the digging works and before casing insertion in the borehole.

3.3 Mechanical behaviour

Several small-scale, in-situ experiments have been carried out in the URL since 2010 to define the process of mechanical loading of the HLW metallic liner parallel to σH (see 3.2). The excavation tests in the URL show a damage zone of the rock at the periphery of the structure. The geometry of this damaged zone is significantly anisotropic, as shown in Figure 13 for an HLW cell parallel to σH: it has a generally elliptical shape with its largest extension along the horizontal. The damaged area presents itself as a fractured environment, so that its mechanical characteristics are inferior to those of sound rock. The rock deforms more rapidly along the horizontal than the vertical.

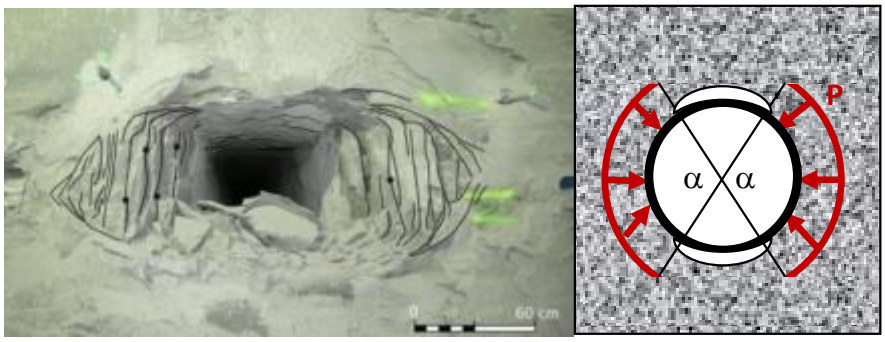

Figure 13: Network of fractures at the periphery of a non-jacketed HA cell parallel to the major horizontal stress (left) and schematic representation of the mechanical loading of the lining that results in the short term (right)

Bumbieler et al. (2015) [5] proposed (Figure 14) three phases during loading. In the first, radial load is localised in the horizontal direction corresponding to the maximum extension of the excavation-induced fracture network. This loading results in a radial bending of the tube and the maximum ovalisation reaches 1% of the diameter of the tube. Once the annular space is taken up at least in the vertical direction, the mechanical load remains anisotropic with no impact on tube convergence. This second loading step is followed by a third, corresponding to a progressive decrease in load anisotropy, resulting in a decrease in ovalisation. Mechanical signatures of the loading applied by the rock (i.e. the evolution of the circumferential strain $\varepsilon\theta\theta$ around the inner face of the casing) confirm the loading anisotropy. Indeed, by comparison with a theoretical symmetrical anisotropic load, it can be seen that the maximum load axis is almost horizontal

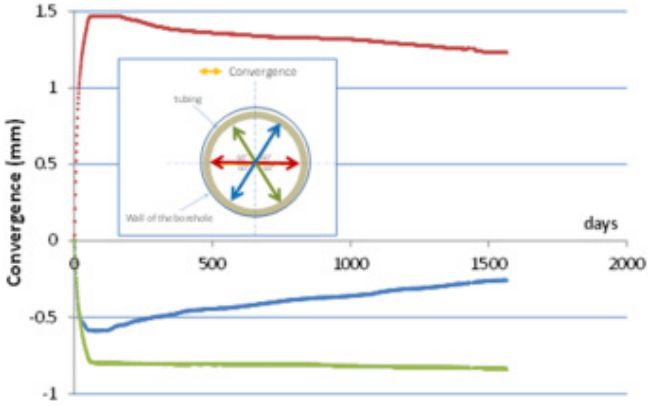

Figure 14 : Convergence of the casing in a borehole (Bumbieler et al., 2015).[5]

Figure 15 shows the evolution over time of the ovalization of a reduced scale steel casing and a full scale 1: 1 scale casing (in both cases the bending stiffnesses are equivalent). On a smaller scale, due to a smaller initial annulus and a more regular drilling geometry, the annular void was resumed in the vertical direction in less than 100 days, resulting in the blocking of the ovalization of the tubing. On a 1: 1 scale, however, the annular clearance is still not resumed in

the vertical direction on 3 of the 4 measuring sections, which explains the continuation of ovalization of the liner after more than 3 years.

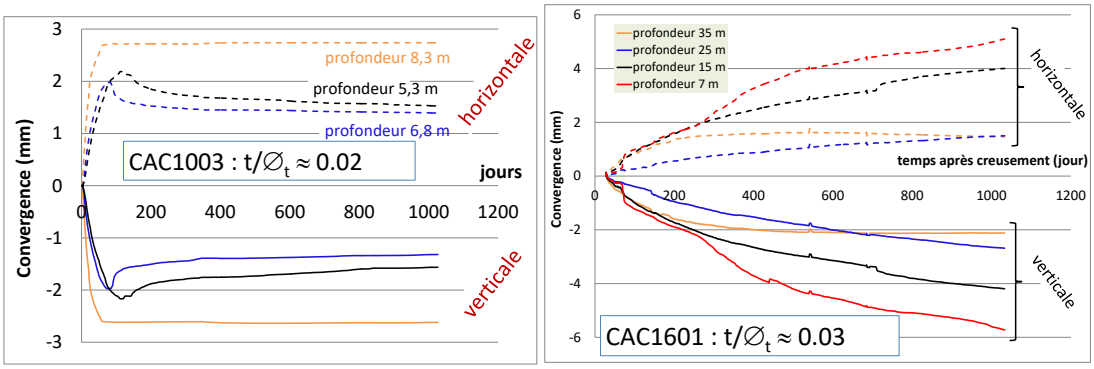

Figure 15: Evolution of ovalization of a 1: 5 scale casing (left) and a 1: 1 scale casing (right) at different depths (t = thickness, □t = diameter)

An extrapolation of the curves on the right of Figure 15 shows that the maximum ovality at 100 years is of the order of 10 mm for an initial diameter of the order of 700 mm. This estimate is consistent with numerical simulations of the long-term mechanical behavior of liner made elsewhere (not already published).

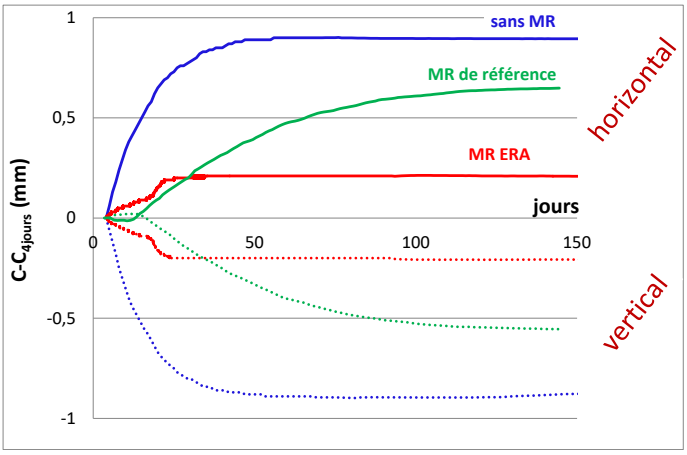

Figure 16 : Convergence of steel casings with filling material type ERA, with filling material of reference and without filling

The monitoring of the convergence of the lining of the cell CAC1602 whose initial annular void was filled with the grout cement / bentonite [6] shows that its ovalization continues after 2 years. **It will be noted that this is reversed compared to that measured on liners without filling** (ie vertical convergence and horizontal divergence, see Figure 16), highlighting a scaling effect with respect to the behavior of casing CAC1102 (flexural rigidity and identical filling material). At a 1: 1 scale, the injection of a cementitious filler material between the rock and the liner thus modifies the ovalization process. In this case, it is no longer linked to the presence of annular vacuum in extrados of the liner (which has been filled), but only to the variability of the deformability of the damaged area: it is deformed more horizontally vertical and ovalization is done horizontally. However, the kinetics of ovality seems to decrease compared to that measured without filling (lining of cell CAC1601, see Figure 20). This scale effect is not reproduced today by the various numerical simulations carried out

4 AHA1604 Demonstrator

The alveolus AHA1604 was excavated in GAN gallery in Andra's URL between Nov 9th and 16th, 2017 see Figure 17.

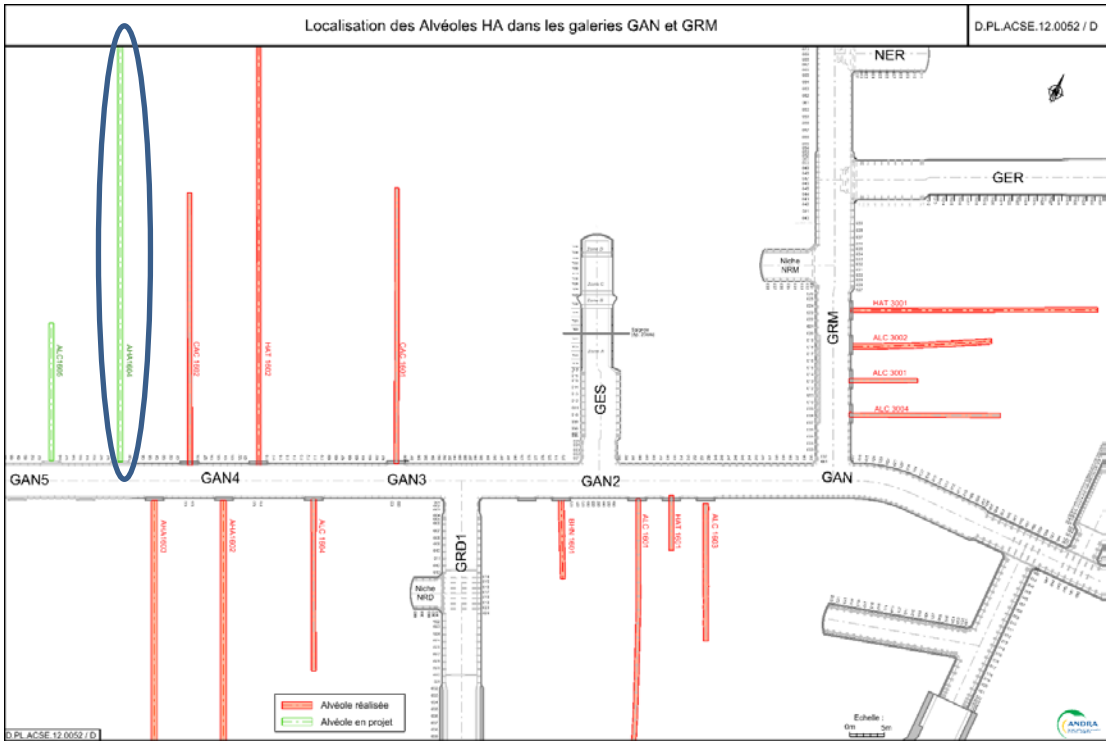

Figure 17 : localization of AHA1604 demonstrator in the GAN gallery

4.1 AHA1604 main objectives

The main objectives of AHA1604 was to shown the possibility to dig and set up a very long cell (>100m) with the new concept of HLW cell using the filling material

4.2 AHA1604 monitoring objectives

AHA1604 also makes it possible to test the feasibility of installing optical fiber to monitor strain and temperature at the external part of the metallic liner

- a longitudinal optical fiber at the external part of the metallic liner were installed

To test an ovalization measurement section on a liner by optical fiber. AHA1604 is the one of the first step to validate the monitoring design.

Several measurement techniques were installed inside the metallic tube: LVDT , Strain gauges, platinum probes to assess convergences and temperatures. This instrumentation is dedicated to scientific objectives, which is not the purposes of this report.

This report focuses only on the envisaged monitoring system for cigeo OFS measurements only

4.3 AHA1604 general description

The drilled depth of the AHA1604 alveolus is 112.5 m, which was a success because the main goal of this demonstrator is to validate the drilling's method and grout injection up to a depth of about 100 m.

Another goal was to test a new sensing systems based on distributed Optical Fiber Sensors (OFS)[2]. The metallic casing, placed into the borehole and covered by grouting materials, has been composed of several 2 m long tubes. The tubes were inserted as schematically presented in Figure 9 with the location of the tubes, numbered from 1 (bottom of the borehole) to 56 (gallery side). The order of the sleeves has been modified in order to guarantee emplacement of tubes 51 to 55. These sleeves were equipped with OFS cables and had to be installed in the borehole, in spite of breakout existing, very early after excavation in the borehole, which could make casing insertion stopped at any depth.

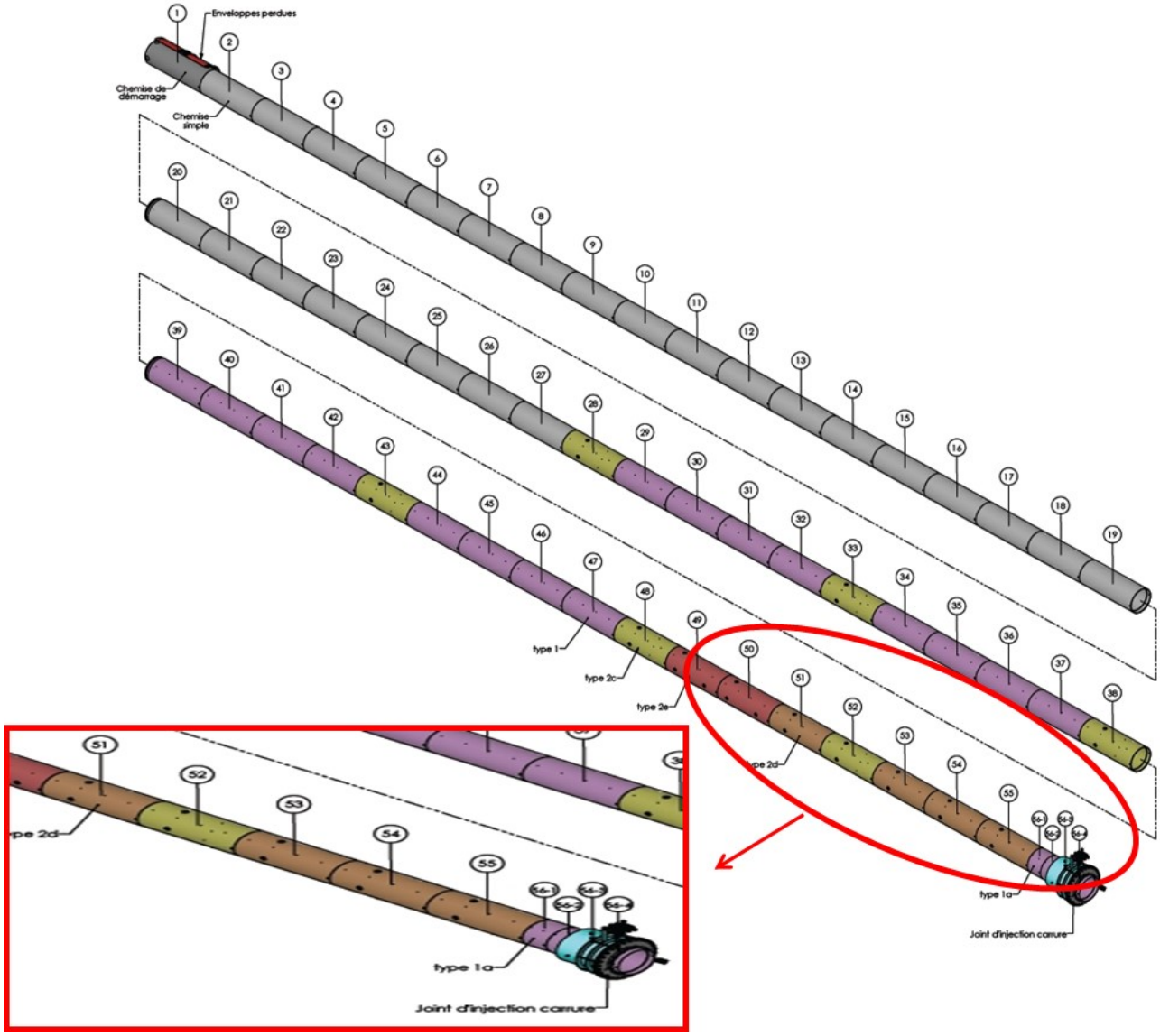

Figure 18: AHA 1604 – scheme of connections and numbering of individual casing segments (sleeves)

4.4 Optical fiber instrumentation description

The aims of this installation were to test several patterns of OFS cables:

- coiled and glued on the external face of the metallic tube for ovalization measurements;
- placed longitudinally for strain and temperature measurements:
  - glued every 2 m in one point at the center of the metallic tube;
  - glued along each tube over about 1.5 m of 2 m metallic tube.

4.4.1 Cable type

The sleeves were in addition instrumented with two types of OFS cables (specifications provided in Appendix):

- Strain sensing V9 (SSV9) from Brugg company used for longitudinal measurements of strains and temperatures. It contains one single-mode fiber optic;
- Emboss FN-SILL-3 (Emboss-3) from Neubrex company, dedicated to ovalization measurements. It contains two single-mode fiber optics;
- Brugg T 85 temperature from Brugg used for longitudinal measurements of temperatures It contains two single-mode and two multi-mode fiber optics.

Each cable has its specific coefficients [3], which are to be implemented in optical interrogators in order to convert raw measurements (classically frequency or power) into physical measurements (strains, temperatures).

4.4.2 Optical fiber measurement unit

The cables were connected to two interrogators, one to Raman interrogator into multimode fibers and one to combined Brillouin and Rayleigh interrogator into single-mode fibers.

The first interrogator is the ULTIMA-S for raman measurement, manufactured by SILIXA. It can achieve perform automatic self-calibration of every measurement against an internal high-precision reference sensor. The ULTIMA-S range, offers a temperature resolution of approximately 0.4°C at a distance of 5km over a period of 1 min for a 12.5cm sampling rate. At longer measurement intervals the temperature resolution can be improved to 0.01°C at the near end and better than 0.03°C at the far end over longer measurement times. Fibre type to be connected is standard Graded Index (GI) 50/125µm multimode fibre. Measurements can both be performed, in single-end and in double end (loop) fibers.

Technical specifications of the instrument are in Appendix.

The second interrogator is NEUBRESCOPE NBX-7020-S. It offers the following types of Brillouin and Rayleigh scattering-based measurements:

- Pulse-Pre-Pump Brillouin Optical Time Domain Analysis (PPP-BOTDA) ;
- Tunable Wavelength Coherent Optical Time Domain Reflectometry (TW-COTDR) ;

and additionally ;

- Optical Time Domain Reflectometry (OTDR) ;
- Brillouin Optical Time Domain Reflectometry (BOTDR).

The OTDR and BOTDR are standard techniques. The former allows one to check the optical fiber installation integrity, while the former provides strain/temperature measurements. It requires single-end fiber access but the measurements resolution is limited to 1 m.

Neubrex developed and patented the PPP-BOTDA technology, which employs the pre-pump light. As all BOTDA based techniques, it requires the double-end (closed loop) fiber access. However, unlike other methods it offers the measurements resolution as high as 2 cm.

In Neubrex TW-COTDR method, the tuneable wavelength DFB laser and frequency scanning are used to obtain power spectrum. TW-COTDR enables single-end access distributed measurements, high sensitivity, covers wide range of spatial resolutions, and can provide

measurements over long distances. The method by principle captures entire frequency-distance data. As the spatial resolution does not limit the frequency scanning range, it can be arbitrarily increased if required due to measured strain/temperature changes of to improve the spectrums cross-correlation. Furthermore, if the fiber length is modified (for example fiber is reconnected, new portion inserted, or repaired in case it was broken) all the previous measurement data is still valid and can be used. This is of crucial importance in any industrial application. The method, however, is relatively slow, and measurement may take up to a few minutes. The speed depends mainly on the distance and frequency scanning ranges. One of the advantages of TW-COTDR is the considerably longer distance range it can cover.

Neubrex instrument claimed to be unique for the association of these varied measurement techniques. It also implements a unique Rayleigh measuring technique, which enables very long-range strain or temperature. What is more, thanks to this association, it provides both strain and temperature distributed measurements [4]. This unique feature is provided over a tens of kilometres range with cm-order spatial resolution. Technical specifications of the instrument are in Appendix.

4.4.3 OFS cables layouts and fingerprinting

As distributed OFS measurements are distributed, each part of the OFS cable is a sensing point, according to the sensing parameters of the interrogator. For instance, for an interrogator's parameter of 10 cm of spatial resolution and 5 cm of sampling interval, we obtain one measurement point every 5 cm and this measurement is an average of 10 cm of the OFS cable.

This very interesting advantage of distributed measurements is offset by the required accuracy on OFS cable localization. Indeed, each metric point (for instance 124.65 m) should be localized in the structure (for instance: between 5.60 and 5.65 m along the tube in the left part). One can easily observe that mistakes on this localization involve wrong interpretation of the behaviour of the monitored structure.

The next sections contain the results of marking the selected key positions along the fiber to allow easier interpretation of the results and possible matching to a 3D geometry of the casing. This process is commonly referred to "fingerprinting".

4.4.3.1 Loop

Sleeve n°51, as the first tube, contains a specific device dedicated to make a loop with each OFS cable, with respect to its maximum pending radius. The loop is required in order to allow short spatial resolution (according to interrogator specifications) for strain and temperature measurements into single-mode OFS cable. Indeed, with open-end configuration spatial resolution is limited to 1 m, when in loop configuration it's possible to perform centimetric spatial resolution.

This device dedicated to loop management is a very important and sensitive part of the instrumentation. It should survive installation, because of expected frictions during sleeves insertion phase, and to maintain the OFS cable with acceptable pending radius over time.

The tested design is presented in Figure 20where one can see the metallic protections and the two OFS cables (blue and red) placed and protected inside.

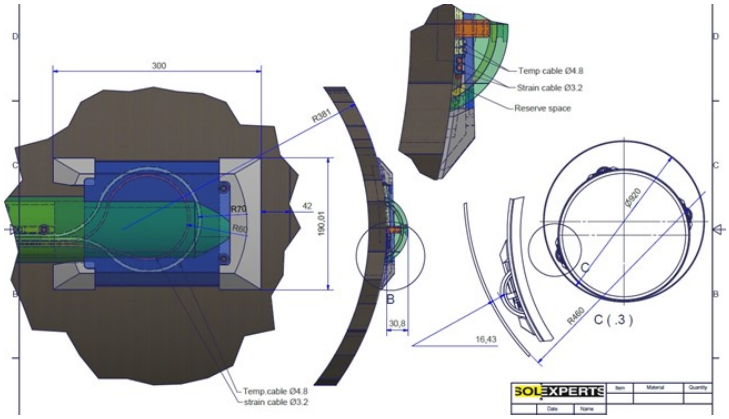

Figure 19 : design of the loop protection

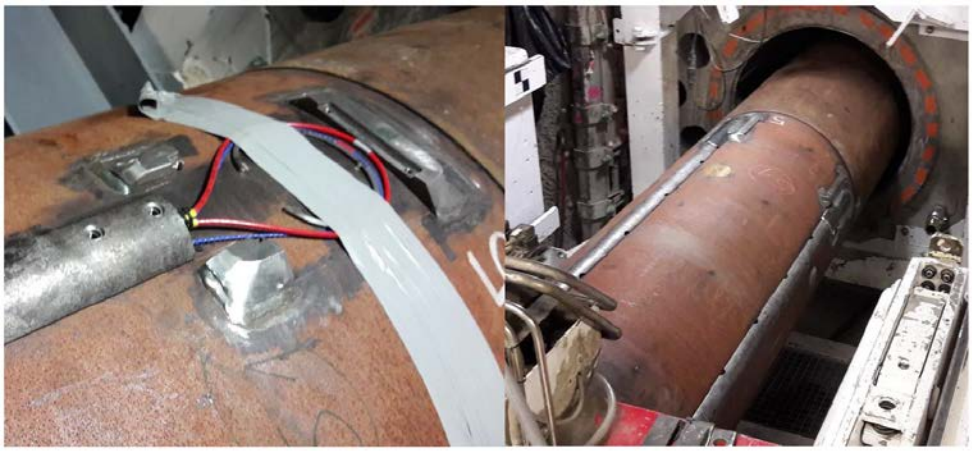

Figure 20: Pictures of loop protection device during in situ installation in AHA1604 demonstrator before closing the protection (left) and after, in final configuration (right)

4.4.3.2 Layout of longitudinal OFS cables

The casing was equipped with longitudinal fibers according to three different orientations. The Figure 21 presents a cross-section of the tube installed in AHA 1604 demonstrator indicating the orientations: 72°, -18° and -108°.

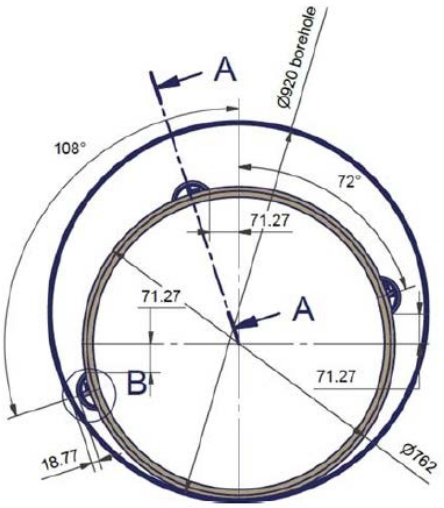

Figure 21: Casing cross-section with the three orientations of the OFS cables.

The OFS cables in longitudinal pattern are installed along guides through tubes 51, 52, 53, 54, 55, 46, 47, 56-1, 56-2, 65-4 (see Figure 21).

The metallic covers are made to allow the grout penetration.The purpose of the measurement is eventually for the heating cells, to follow the expansion of the entire structure after heating.

- Type 1: The cables are glued with a set of cable provided at each sleeve fitting => measurement possible continuously about 1m80 for each jacket, and slack of cables respecting the minimum radius of curvature at the nesting.
- Type 2: stretched between two attachment points (centrally positioned on each liner, 1 attachment point per liner). This solution could allow a measurement of expansion sets but has never been tested in the laboratory and we have no feedback associated with this method. This solution uses the deformability of the fiber / cable (ie 1% elongation possible (over 2m here) according to the manufacturer), to absorb inter-shirt games

.

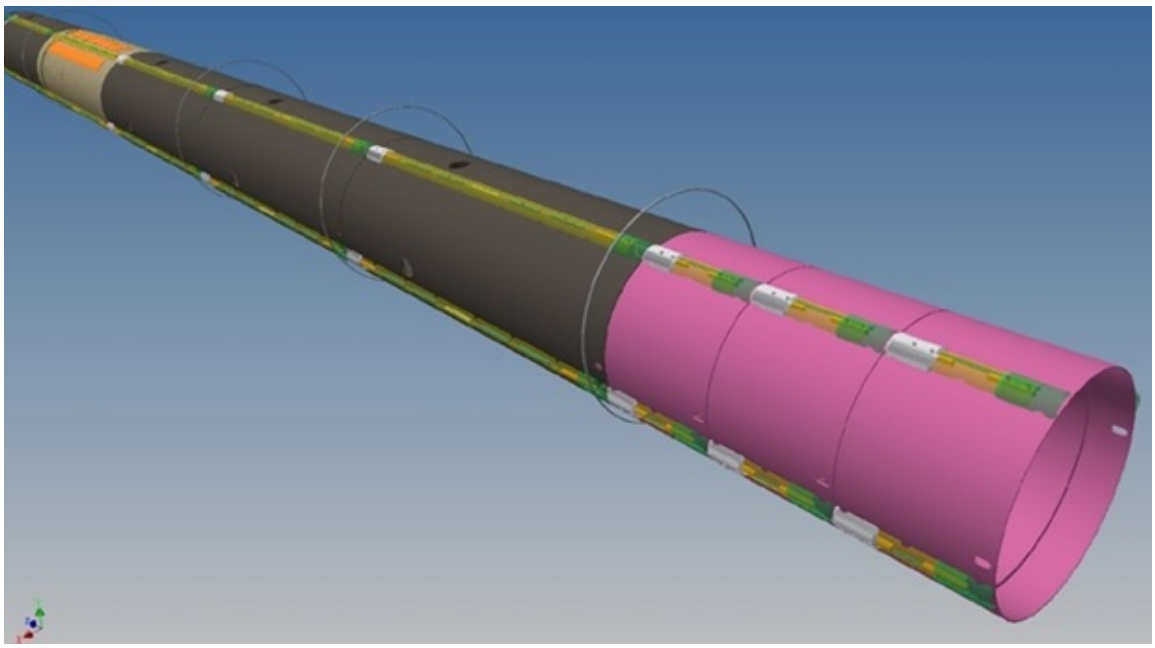

Figure 22: 3D view of the optical fiber configuration on the external part of the AHA1604

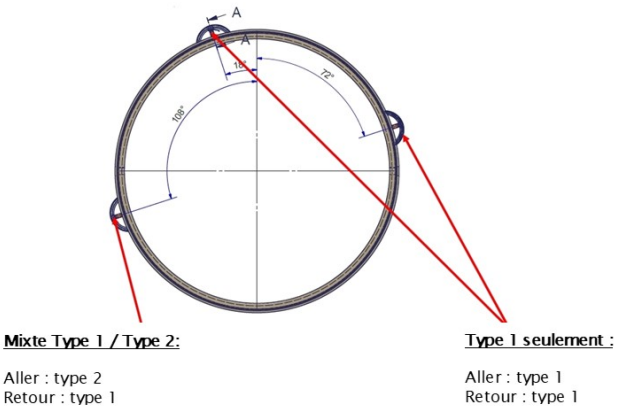

Figure 23 : Alveoli AHA1604: configuration and positioning of measurement channels by longitudinal optical fiber (View from gallery).

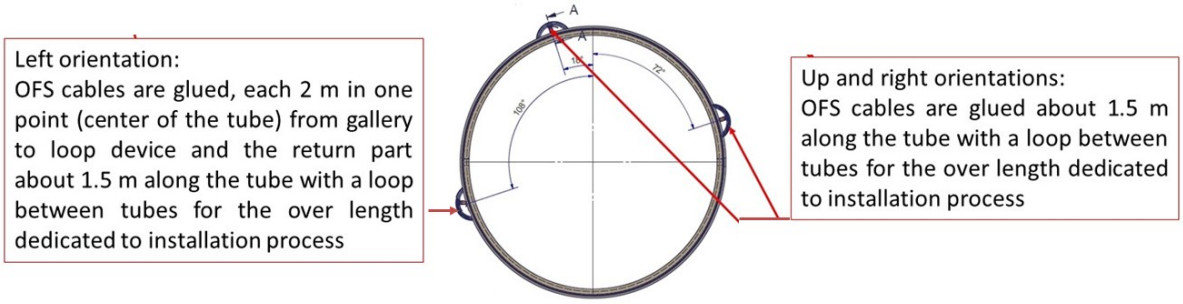

Figure 24: Illustration of the fixation methods of SSV9 cables at the surface of the casing for longitudinal measurements according to the orientation

The installed tubes, from 51 to 56, were pre-fitted with optical fiber modules and covered with protectors to ensure tube installation process. The samples of installed fiber modules are presented in Figure 25 and Figure 26 where it's possible to see the different configurations of fixation for the SSV9 cables.

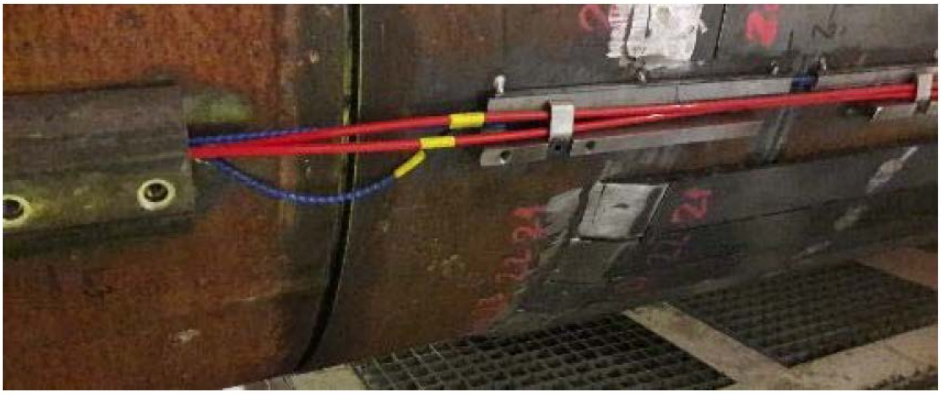

Figure 25: On site longitudinal of installation with two different configurations of fixation for SSV9 cables (blue)

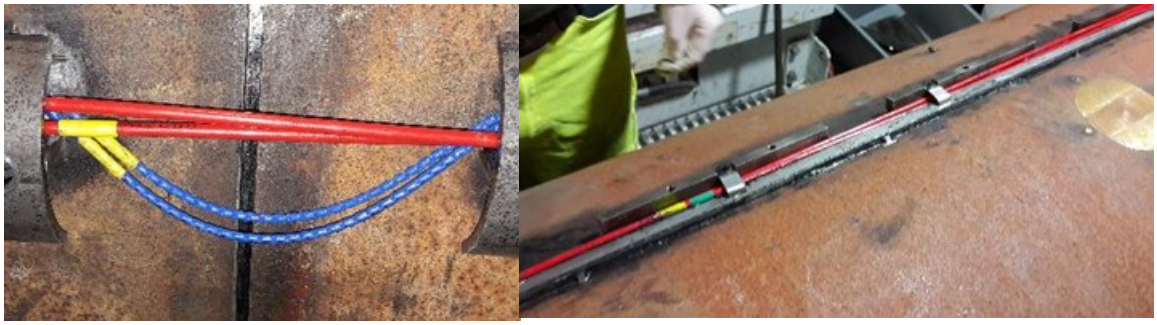

Figure 26: Photos of the longitudinal OFS cable installed at the top (right) and the over length for installation management (left)

Indeed, in the Figure 23 and Figure 24illustration indicates that for the up and right orientations, SSV9 cables were installed, in one configuration, glued along the tube. The glued part is about 1.5 m (see parts KL, MN, OP, RS in Figure 15) along the 2 m tubes. In order to avoid traction on OFS cables, a loop of a few centimeters of over length has been kept between each two forwarded glued sleeves (see parts L M, NO, PR in Figure 15). The left part has been equipped with SSV9 cable glued in the middle of each tube in one point (see parts E, F, G, I in Figure 15) in order to provide information as a long-based extensometer.

4.4.3.3 Fingerprinting of longitudinal OFS cables

Fingerprinting of longitudinal SSV9 cable <u>at left location</u>

The coordinates of key points are mapped to the tubes geometry and presented in Figure 27.

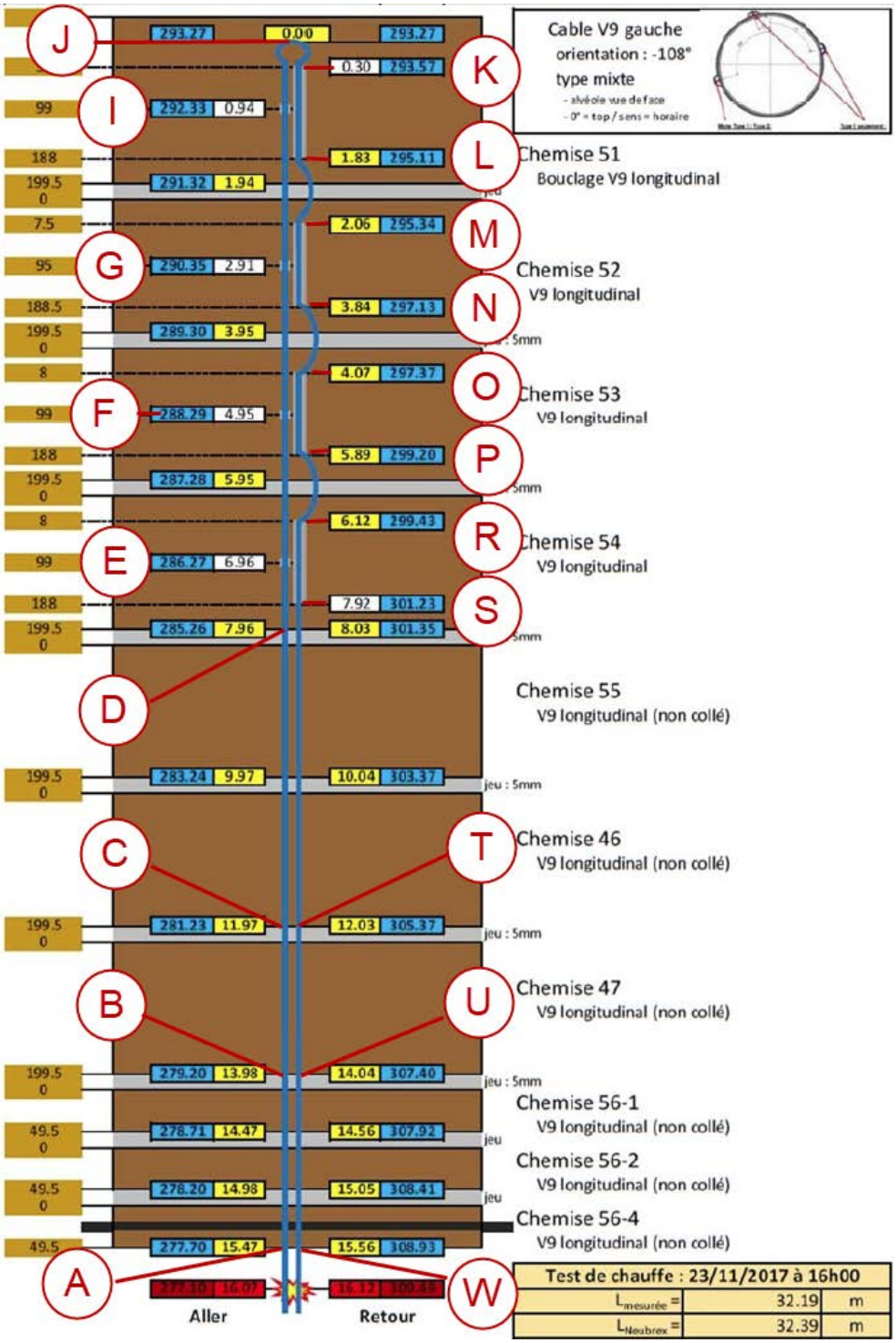

Figure 27 SSV9 left – layout after installation

This layout is for long term monitoring. However, during installation process itself, an additional communication fiber **55.53 m** long. This means that during the sleeves insertion process, the fiber coordinates are shifted by this distance. This configuration has **<u>only</u>** been used during installation process and then configuration in Figure 27 has been implemented.

Fingerprinting of longitudinal SSV9 cable at up and <u>right locations</u>

The coordinates of key points are mapped to the tubes geometry and presented in Figure 28.

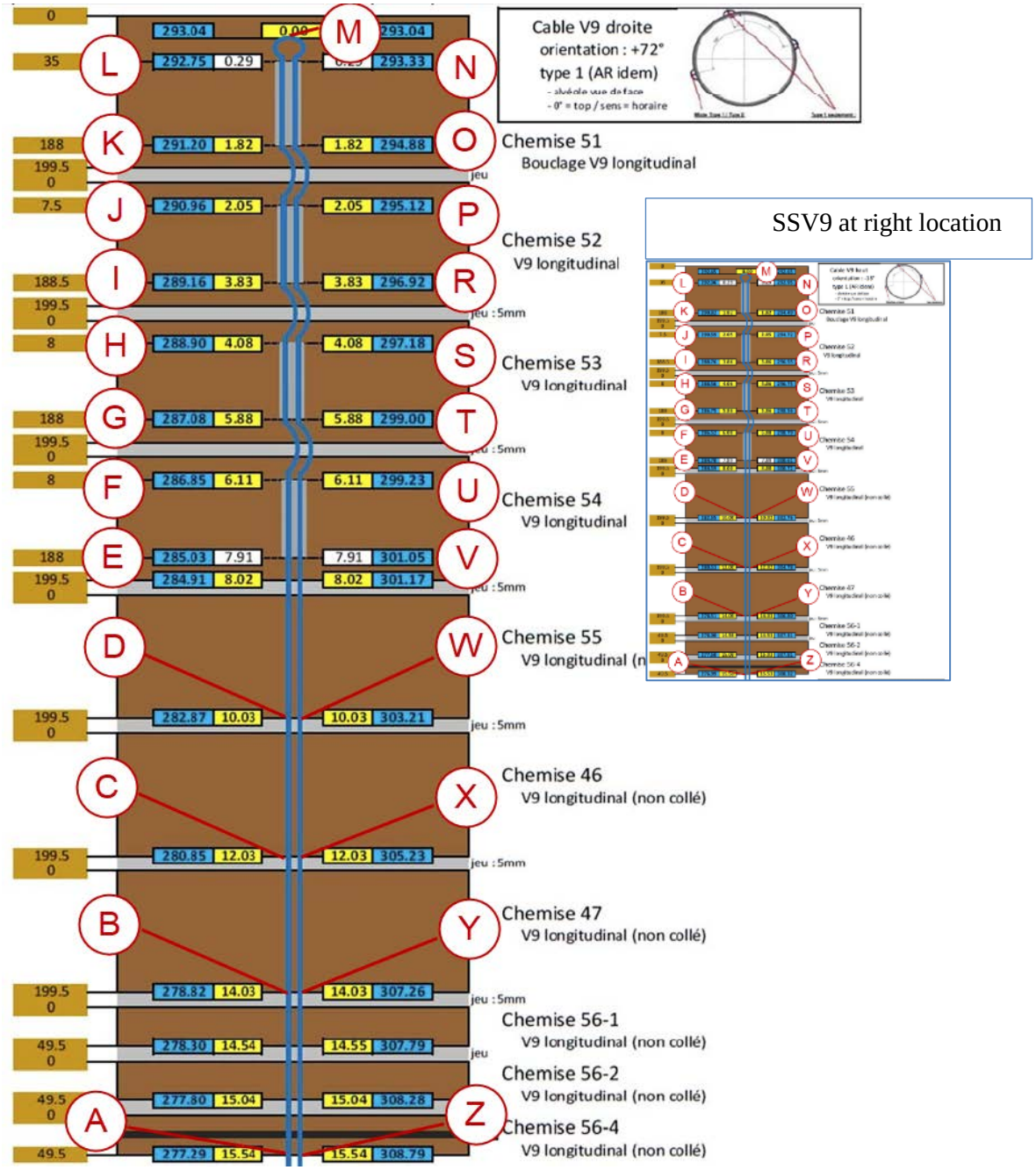

Figure 28: SSV9 cable Up location and (in small size – right) at the right location layout after installation

In Figure 28 several parts of the OFS cable are glued, for instance EF, GH, UV segment, over about 1.5 m. the remained part are note glued in order to manage tubes insertion operations and potential traction at the cable.

4.4.3.4 Layout of ovalization OFS cable

Sleeve n°52 was design (see Figure 26) to test the ovalization detection by distributed OFS cable glued spirally at the external surface of the sleeve. This is clearly depicted in Figure 29, where the glued Emboss cable, in five loops separated by 28 cm, is visible prior to covering OFS cables with protective strips. They consist of several metallic plats, put around the tube in order to avoid damage on the fiber during insertion phase in the borehole. The OFS cable was protected at the beginning and at the end parts of the spirals to avoid direct contact or hit during manipulations and transfer work.

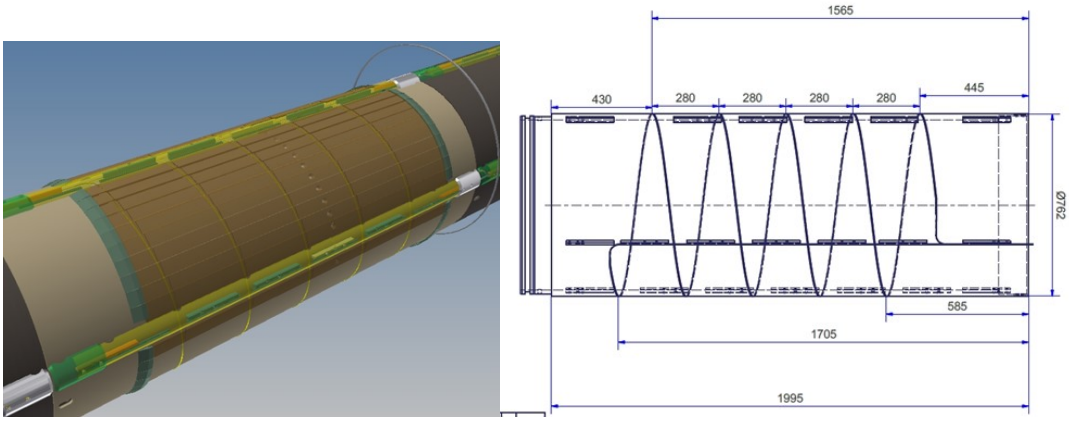

Figure 29 : Design and characteristic of the Sleeve n°52 for ovalization measurement

Figure 30: picture of the sleeve n°52 without (left) and with metal proctection plate .

4.4.3.5 Fingerprinting of Emboss-3 cable for ovalization measurements

The coordinates of key points are mapped to the tubes geometry and presented in Figure 31

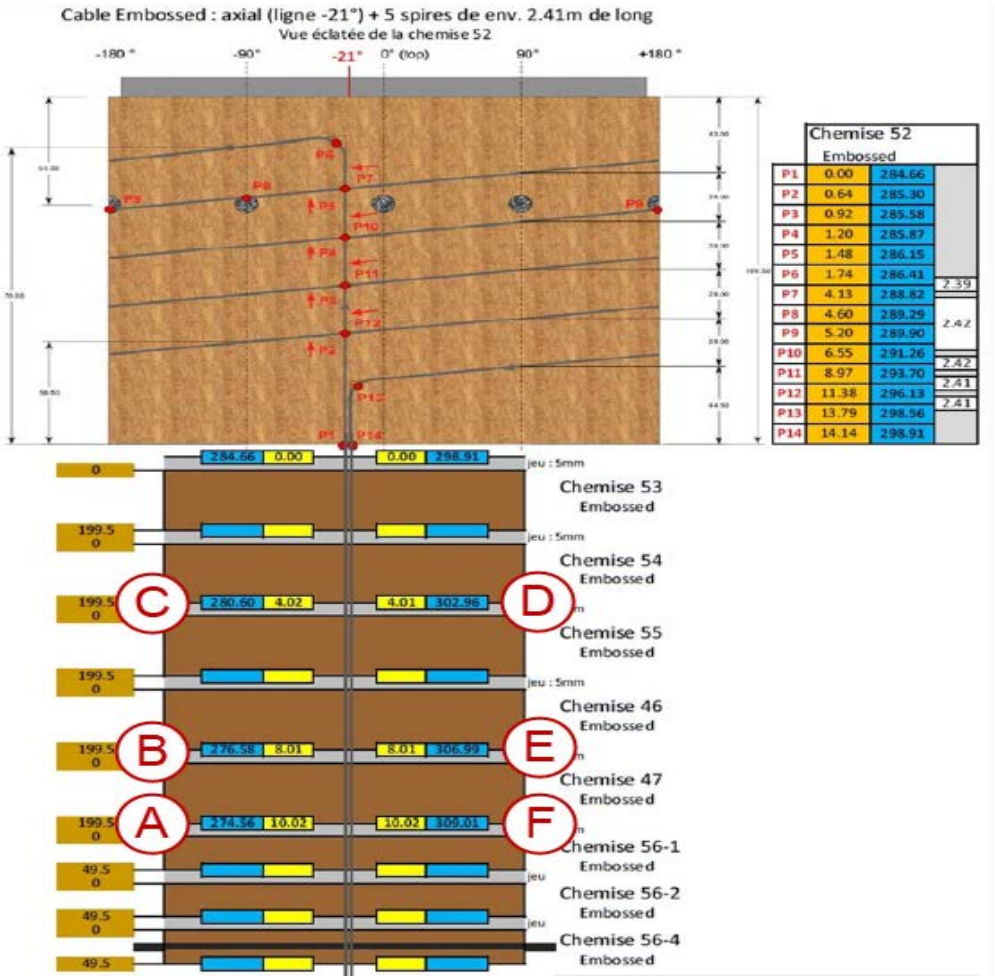

Figure 31: Emboss-3 cable layout after installation with specific localizations (table)

4.4.4 OFS acquisition configuration

The sensing system was composed of several optical lines. Each line was composed of:

- The sensing part is localized in the structure to be monitoring (at external face of the tubes);
- The communication part, where classical optical fiber cables allow connections between the interrogators, placed further in a dedicated gallery about 200 m, and the interested part in the alveoli inside a junction box.

Both galleries are connected together by several OFS cables, named hybrid OFS cables.

All OFS cables (dedicated to monitoring) were assembled in one junction box (see Figure 32) where they are connected to communication cable (hybrid cable). This cable connects two junction boxes (BOX AHA1604 and BOX GAN-GRD) where the second one allow to attend the optical interrogators few hundred of meters far in G10 gallery. The interrogators were placed in a “clean room” to protect them, especially from ducts largely spread in underground area.

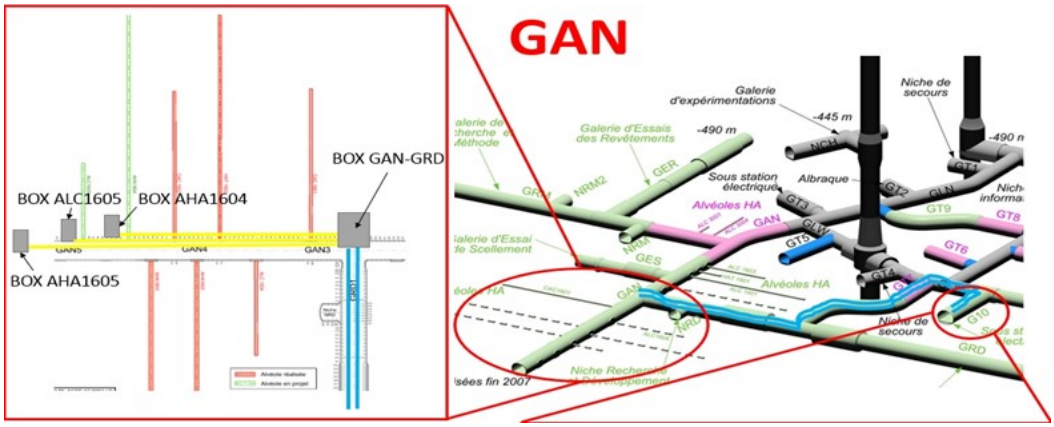

Figure 32:Localization of the demonstrator in GAN gallery and the positions of the OFS instruments in G10 gallery (right) and the position of connection boxes for OFS cables (left)

The instrument, optical switch, and control unit were installed in dust-proof box, shown in Figure 2.

Figure 33. Dust-proof box with monitoring system components

4.4.4.1 Optical line scheme

The Neubrex interrogator has been connected to OFS cables according the following:

- Channel 1: Brugg cable V9 placed at the left orientation of the casing;
- Channel 2: Brugg cable V9 placed at the up orientation of the casing;
- Channel 3: Brugg cable V9 placed at the right orientation of the casing;
- Channel 4: Neubrex cable Emboss-V3 placed in spiral for ovalization measurement.

The Silixa interrogator has been connected to OFS cables according the following:

- Channel 1 : Brugg cable T85 placed at the left, connected to the up and then to the right orientation at the casing.

The Figure 34 presents the connection scheme for the lines *in situ* with each type of link:

- Pigtail: for connections *via* Patch-cord with connectors type FC/ APC at each side;
- SPL: for splices performed between two optical fibers;
- SM: for single-mode fiber;
- MM: for multimode fiber;
- Colours: indicating in each cable the color of the coating covering the fiber optic.

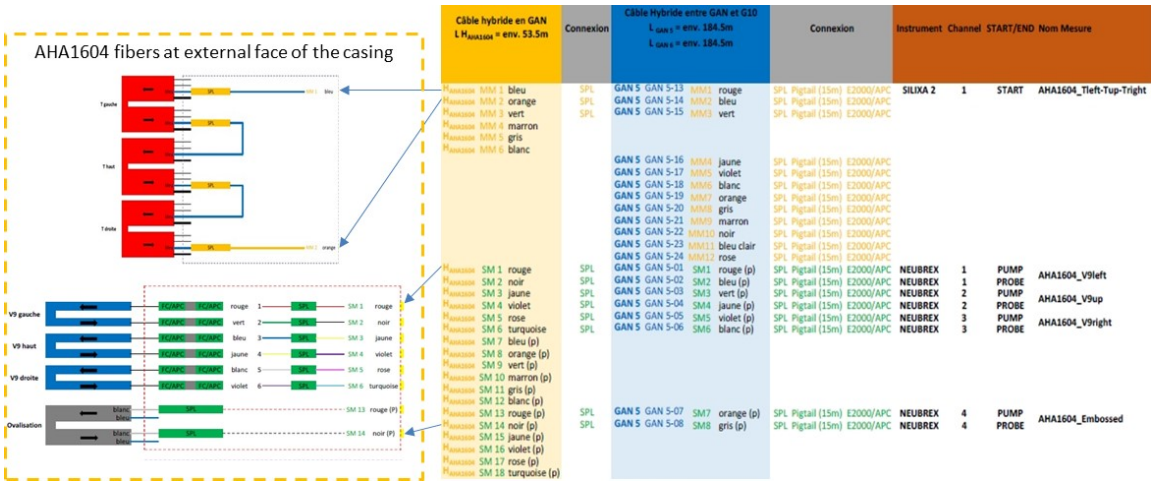

Figure 34: Optical fibers and switch connection scheme to Neubrex and Silixa interrogators

This connection scheme shows that for each optical line several fibers are connected together. These connections can involve losses and uncertainties in localization, which can be reduced by an accurate fingerprinting.

4.4.4.2 Configuration

During installation and subsequent grouting of the gap between the host rock and the casing, the monitoring used the PPP-BOTDA method to capture the strain distribution. Then configuration has been modified for long term monitoring. All these configurations are listed in Table 4.

Table 3 hardware settings during installation, grout injection and for long term monitoring

example of channel 2	**Installation**		**Injection**		**Long term**	
Parameter	PPP	TW-COTDR	PPP	TW-COTDR	PPP	TW-COTDR
Distance range [m]	800	-	600	-	600	600
Spatial resolution [cm]	20	-	20	-	10	10
Sampling interval [cm]	10	-	10	-	5	5

Average count [-]	2^{13}	-	2^{13}	-	2^{15}	2^{13}
Pump output power [dBm]	+3	-	+3	-	+1	0
Probe output power [dBm]	+30	-	+30	-	+27	+28
Frequency start [GHz]	10.0	-	10.0	-	10.25	194000
Frequency step [MHz]	5	-	5.0	-	2.0	200.0
Frequency count [-]	201	-	201	-	401	2001
Frequency end [GHz]	11.0	-	11.0	-	11.05	194400

4.5 Measurements results on AHA1604 demonstrator

The first results obtained in situ were analysed for several purposes. Installation data required to show if, during the installation process when tube insertion is performed, the OFS cables faced important strains because of the construction method.

During the grouting step, data was intended to help to assess the filling quality of the injected material.

Finally, long-term data will validate ovalization assessment, longitudinal strain and temperature measurements, installation method and robustness.

4.5.1.1 Results during installation process

This section contains measurement results obtained during installation (tube insertion) process. Data is plotted and presented using several types of plots, namely, distribution along the distance, space and time contour as well as function of time at selected locations. In most of the plots the distance coordinates are expressed in both fiber and container tube coordinate systems.

Plots present the values of measured strain as well as the relative strain changes. In the latter, the first measured distribution is used as a reference.

4.5.1.2 Prelimenary results

The strain, as a function of distance, for all monitored tubes is presented in Figure 35, while change over time is shown.

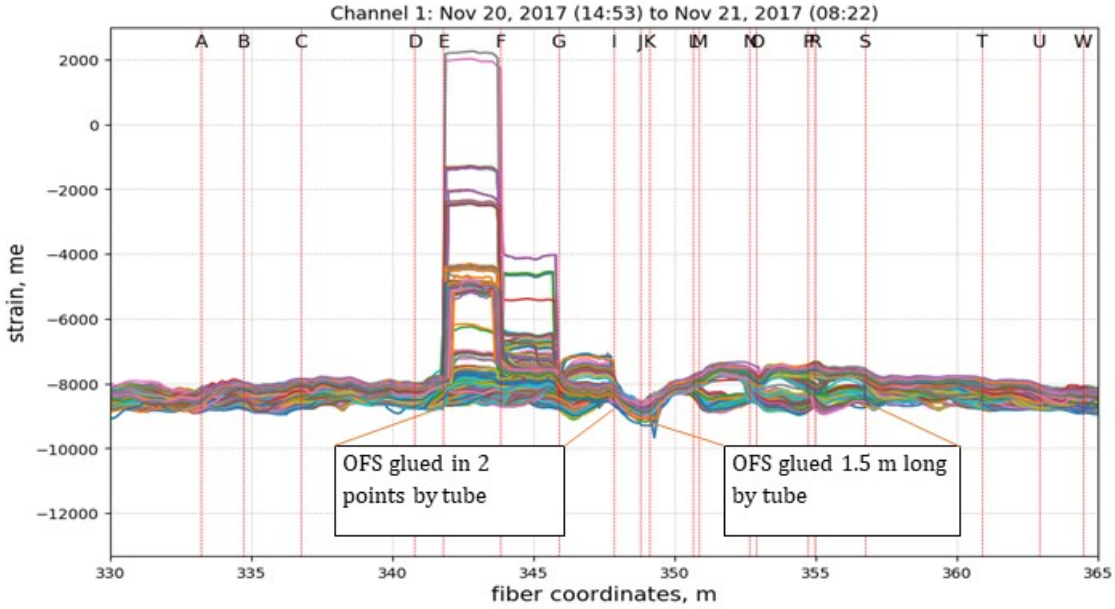

Figure 35: strains along the fiber on the AHA1604 tubes

The strain change for the entire sensing part of Channel 1 cable is shown in Figure 36. The following Figures present each selected segment separately, providing data as both function of time and location. Additionally, the strain trend over time is plotted as specific locations.

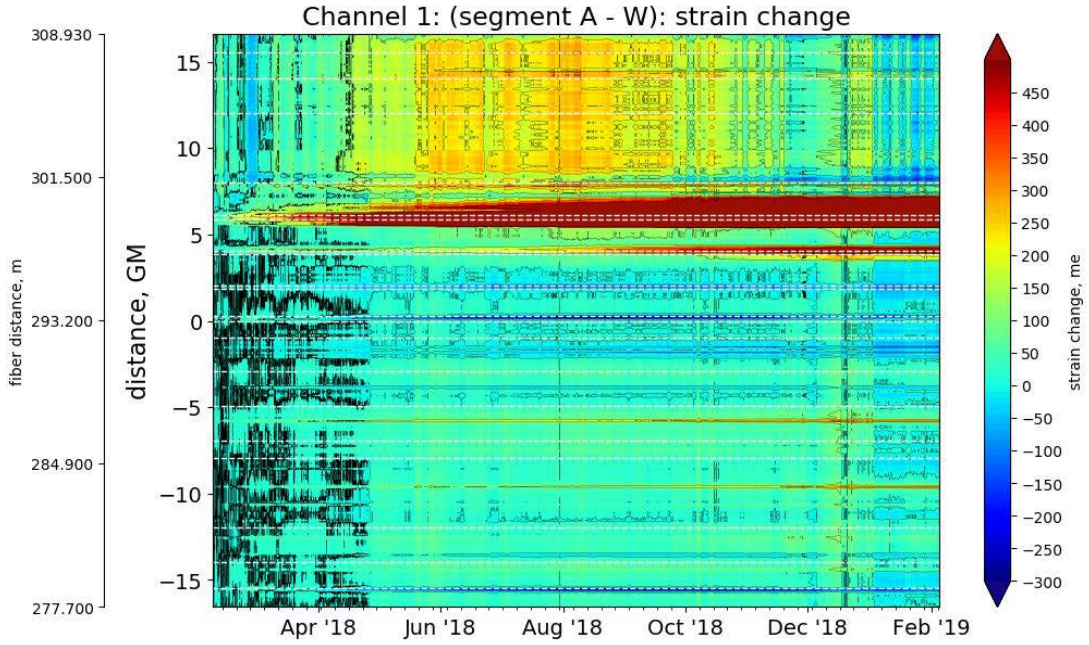

Figure 36: strain change in entire sensing part of the cable V9 left as a function of time between the point A and W (see map on Figure 28)

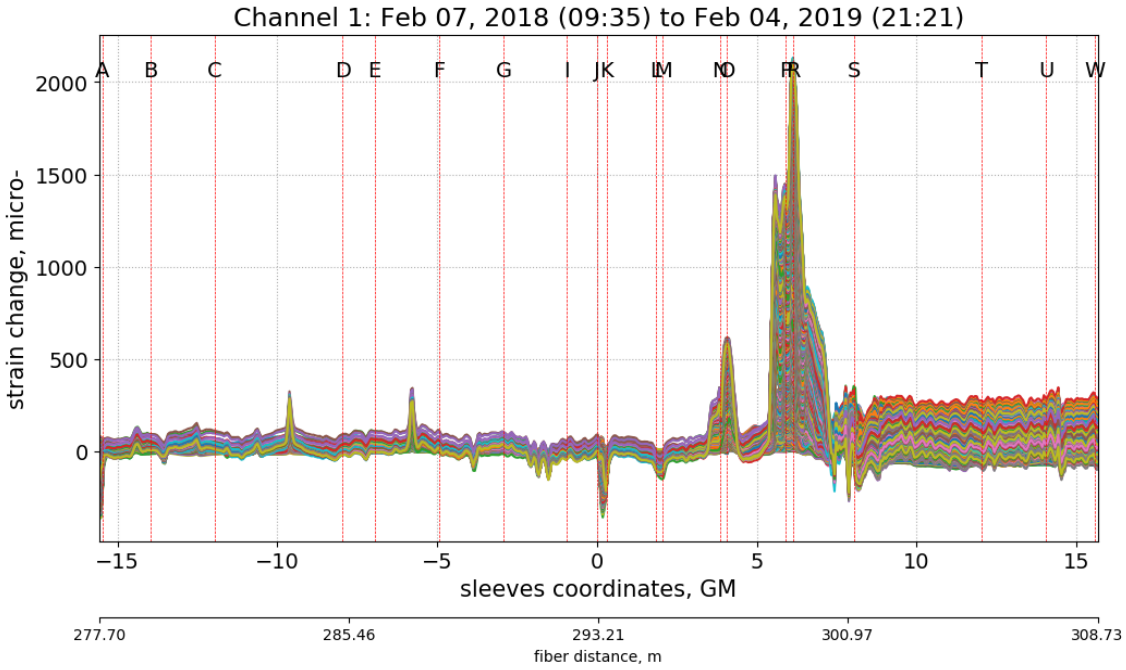

Figure 37: strain change in entire sensing part of the cable V9 left as a function of distance

If we zoom on a specific part of the installed OFS cable at the left side, equipped in 2 different methods, we can see different information. Firstly, at the glued in 2 points OFS cable, as a long based extensometer (Figure 32), strain changes occur immediately and stay, more and less, stable over time. Secondly, for tubes glued along the tubes, observed strains are stable during insertion process (see. Figure 24).

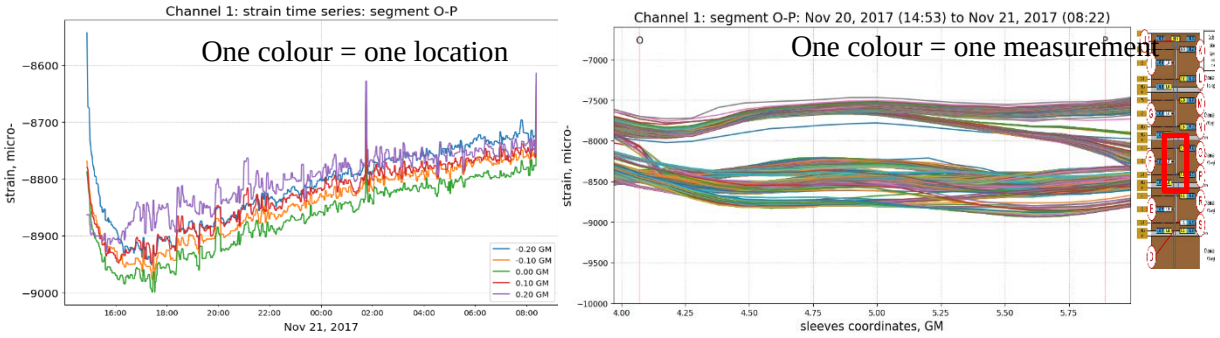

Figure 38: strain on tube as a function of time (left) and as a function of distance (right) at selected locations (segment O-P) where OFS cable is glued at 1.5 m long

1.1.1.1 Strain distribution during grout injection

The construction process consists of digging then inserting tubes and finely injecting cement grout in the surrounding area between rock and casing. In order to check whether the grout injection process can be detected, strains were measured during this phase.

The strain distribution and strain change over time, as a function of distance for all monitored tubes, is presented in Figure 25.

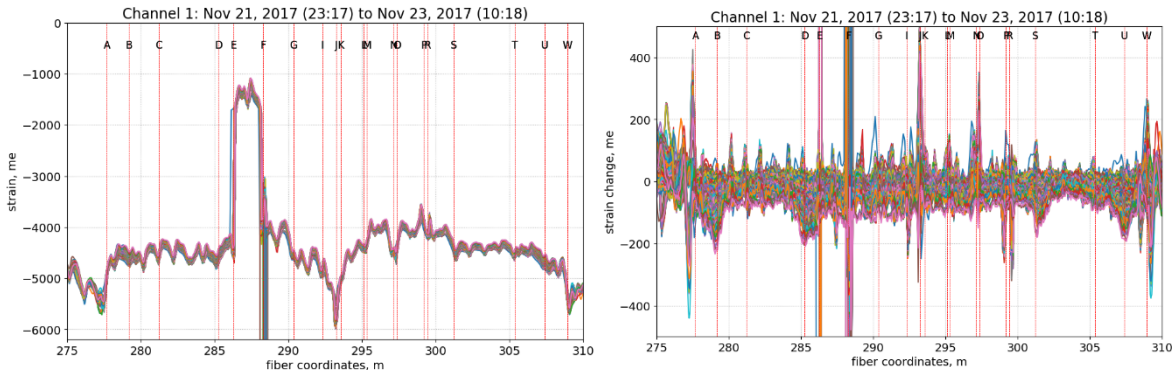

Figure 39: strain distribution (left) and strain change (right) during injection

5 ALC1605 demonstrator

The excavation of the alveoli took place the 15th of November 2018 and has been instrumented between the 19th and 24th of November 2018 in gallery GAN (Figure 19).

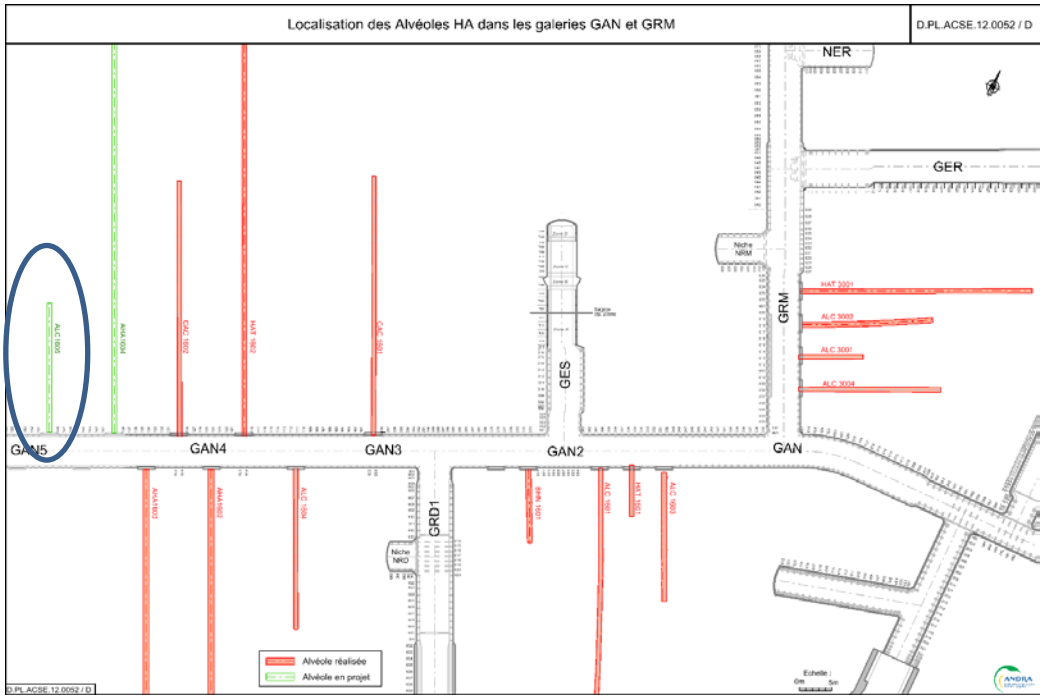

Figure 40: LOCALIZATION OF ALC1605 DEMONSTRATOR IN THE GAN GALLERY

The next step consists of inserting heater in the casing, 15 m long from the bottom, planned mid-2019

5.1 ALC 1605 main objectives

The main aim the ALC1605 experiment is to study the behavior of an HLW cell conforming to 2015 reference concept under solicitation thermal using a heater system. The objectives can decline as follow:

- Study the impact of thermal loading on the thermomechanical behavior of the metallic liner in the presence of filling material (direction and amplitude of ovalization, time to reach the blocking, axial thermal expansion, possible discharge). These data will complement those obtained in the context of the AHA (no thermal loading) experiment to improve the description of the rock / structure interaction in the modeling of the long-term behavior of the HA liner in order, in particular, to verify the gap distance for the package handling.
- Studying the impact of thermal loading on the THM behavior of rock in the field near (but beyond the damaged area) and far (beyond a few diameters) in presence of filler material. It is essentially a matter of following the evolution of Temperature and interstitial pressure fields around the cell and at different distances from the access gallery. A comparison with the measurements made on ALC1604 (previous experiment) will identify a potential impact of the filler material on the kinetics and amplitudes of thermal overpressures in the near or even distant field. We will also look the evolution of the permeability over time to study the damage

5.2 ALC1605 monitoring objectives

ALC1605 is the second step for the qualification of the monitoring system design for the HLW concept.

The main objectives were (i) to qualify the measurement technique, (ii) to validate the design and installation method in situ, (ii) to compare OFS data to reference sensors and to assess system durability, and potential drift, over several years on thermal experiment. In details, the experiment give us the opportunity:

- Consolidate the optical fiber monitoring system to monitor temperature and strain under heat condition
- Compare ovalization measurement by optical fibers to vibrating wire section
- Test geochemical measurement

5.3 ALC1605 demonstrator description

5.3.1 ALC1605 features

The characteristics of ALC1605 are:

- A total length of 28.5 m, including a 6 m cell head and a 19 m "useful" part, with a 1 m overlap area between the liner and the insert;
- Excavated cavity head diameter 791 mm, with insertion of a diameter insert outer 767 mm (an annular space of 12 mm radius) and thickness 21 mm;
- The useful part excavated in diameter 750 mm, with the installation of a liner of diameter outside 700 mm (an annular space of 25 mm radius) and thickness 20 mm;
- A bottom plate, a plate at the top of the liner and a plate at the top of the insert;
- The completion of the heating over a length of 15 m between 10 and 25 m deep

5.3.2 HLW concept evolution for ALC1605 demonstrator

The 2m tube sleeve have followed an evolution compared to AHA1604 demonstrator :

- They are now equipped with centering devices and skates.
- The anti-rolling device has also evolved,

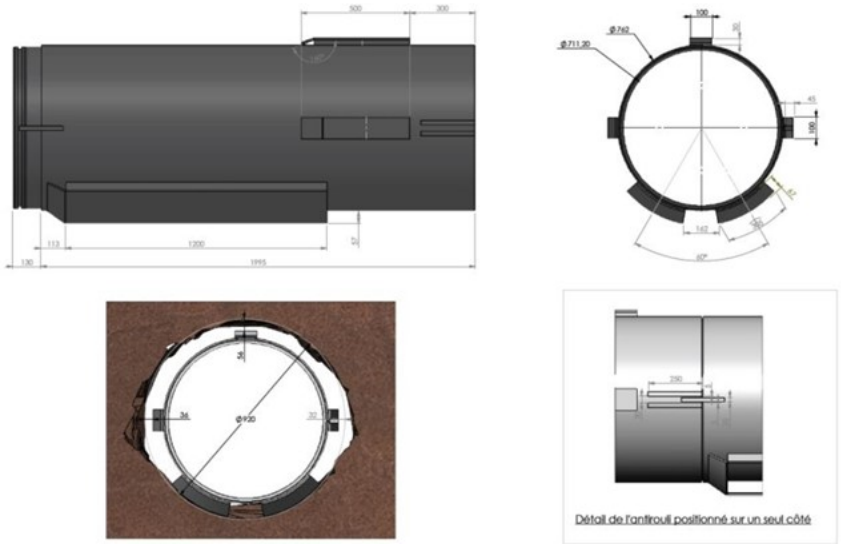

Figure 41: Drawing of the new HLW sleeve with centering element , skate and new type of anti-roll

The new concept has led to some modifications to instrumentation, which will be detailed later in this report.

5.3.3 Heating system

The heating elments will be installed later in 2019. They are not installed yet.

The heating will be carried out using 5 heating elements 3 m long and 508 mm in diameter with power regulation. Each element includes 2 electric resistances to ensure the redundancy of the system. Their installation in the liner will be ensured by 6 transfer pads in high-strength plastic nested in metal parts themselves welded to the body heating (Figure 34). The position of the heating elements in the liner will be very slightly off center 2 mm down.

Figure 42: View of a heater element during installation on ALC1604 (left) – View of a heater/sleeve distance variation sensor section (right)

5.4 Previous results without the filling material (ALC1604)

Details on the ALC1604 experiment can be found here [7]

The main heating phase was launched on April 18, 2013 at a constant power of 220 W / m on the 15 m occupied by the heating elements, between 10 and 25 m deep in the cell. This power was calculated to reach 90 ° C at the external part of the metallic liner after 2 years.

Figure 43 shows the evolution of the lining temperature measured on the internal face at the level of the upper generatrix thus the axial thermal profiles in vault and facing along the in February 2015, January 2016 and May 2017. It is observed that the temperature profile on the side of the liner remains about 4 ° C lower than that measured vault. This difference can to be explained both by the convection inside the lining but also by the influence of boundary conditions around the liner (the contact of the liner with the rock is not homogeneous on its periphery and more important in the horizontal direction as shown orientation of the load). The maximum temperature is located around 18 m deep, so at center of the heated area between 10 and 25 m.

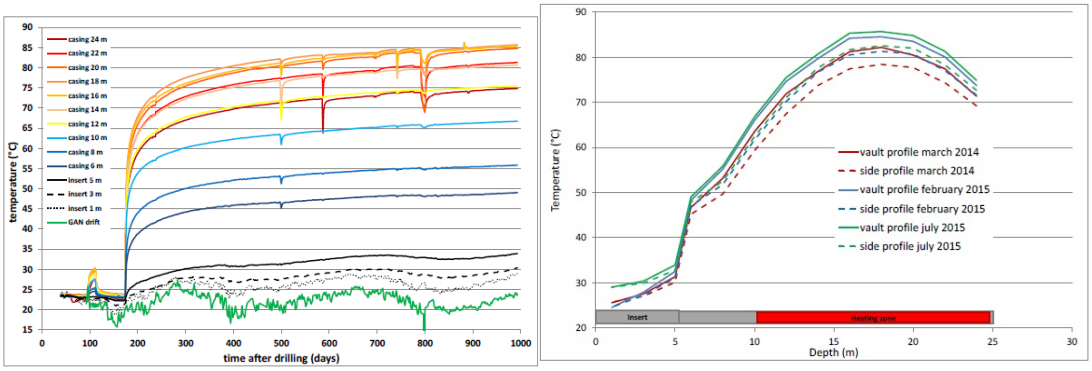

Figure 43: Temperature evolution in the vault of the sleeve (left) and axial thermal profile in the vault and on the side of the sleeve at various dates (right

5.5 Monitoring system description

ALC1605 was instrumented to the extrados of the liner by:

- two systems for measuring the convergence of optical fiber folders (Shirts No. 7 and 9)
- three generators equipped with fiber-optic sensitive cables for the measurement of axial deformations and temperature along the entire length of the cell (folders 2 to 12)
- a temperature measurement section by PT1000 sensors (folder n ° 7)
- a section of measurement of the deformations by vibrating rope (folder n ° 9)
- a cell allowing geochemical measurements (folder n ° 10)

Figure 44 shows the localization of the instrumentation

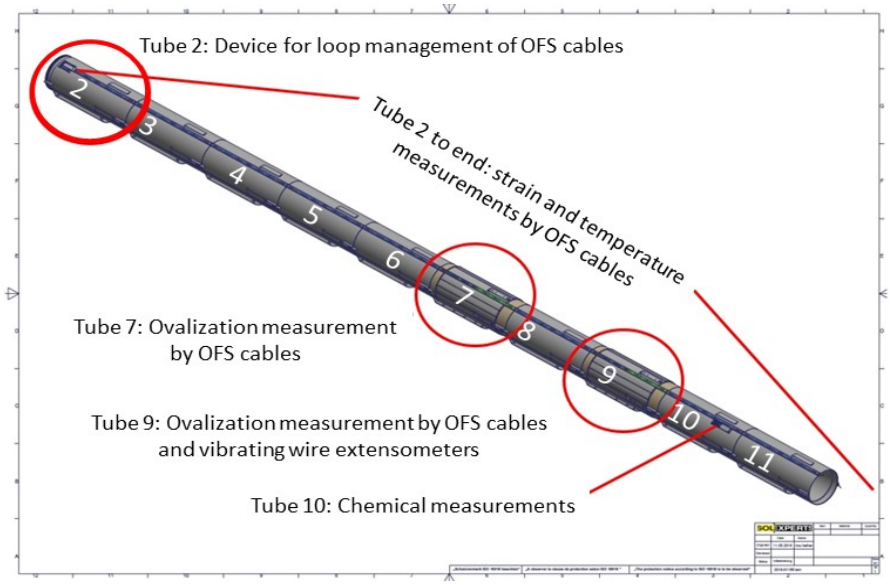

Figure 44: ALC1605 scheme of connections and numbering of individual casing segments (tubes)

5.5.1 Strain and temperature measurement by longitudinal OFS

The purpose of this measurement is ultimately to follow the dilation of the set of the work following the heating of the parcels. It is therefore desired by Andra to carry out distributed measurements strain (and temperature) along the structure.

The goal is always to cover a maximum angular aperture, with a channel on the left as low as possible, a channel on the top and a channel on the right as lower as possible, in order to have a chance to see possible changes in the alignment of the shirts along the cell.

Similar to the first demonstrator (AHA1604), the aims of this installation were to test several patterns of OFS cables:

- coiled and glued on the external face of the metallic tube for ovalization measurements ;
- placed longitudinally for strain and temperature measurements glued along each tube over about 1.5 m of 2 m metallic tubes:
  - With a U shape support to put the OFS cable in and covered by a protection U shaped;
  - OFS cable glued directly at the surface of the casing and covered by a protection U shaped;
  - OFS cable glued directly at the surface of the casing without any support or protection.

The tubes were instrumented with two types of OFS cables:

- Strain sensing V9 (SSV9) from Brugg used for longitudinal measurements of strains and temperatures at one orientation;
- Emboss FN-SILL-5 (Emboss-5) from Neubrex, dedicated to:
  - ovalization measurements ;
  - longitudinal measurements of strains and temperatures at two orientations.
- Brugg T 85 temperature from Brugg used for longitudinal measurements of temperatures.

The cables were connected to two interrogators, one to Raman interrogator into multimode fibers and one to combined Brillouin and Rayleigh interrogator into single-mode fibers.

5.5.1.1 OFS cables layouts and fingerprinting

The following sections contain the results of OFS cables fingerprinting of ALC1605.

5.5.1.1.1 Layout of longitudinal OFS cables

The casing tubes were equipped with longitudinal fibers according to three different orientations. Figure 28 presents a cross-section of the instrumented casing installed in ALC1605 demonstrator.

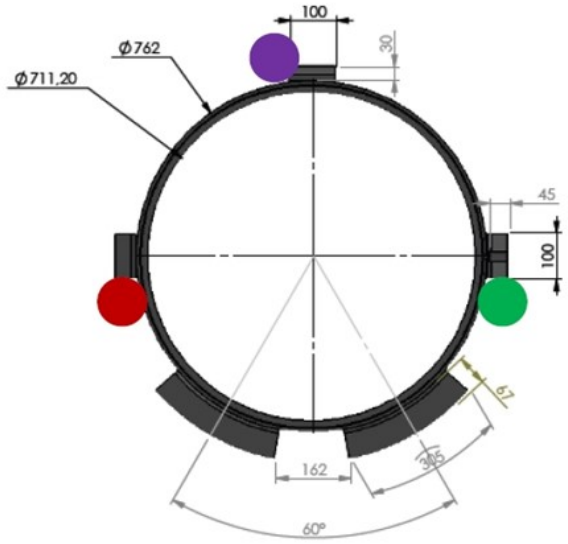

Figure 45: Casing tube cross-section of ALC1605 demonstrator with the three locations of OFS cables (Red, purple and green points)

The OFS cables, in longitudinal pattern, were installed at tubes 2 to 14 (see Figure 46). Tube number 2, as the first instrumented tube, contains a specific device dedicated to make a loop

with each longitudinal OFS cable, with respect to its maximum pending radius. The loop is required in order to allow short spatial resolution.

5.5.1.1.2 Fingerprinting of OFS cables

The coordinates of key points are mapped, similarly to what has been done for AHA1604, with a difference that in this case, the OFS cable has been glued along the entire casing (see. Figure 46).

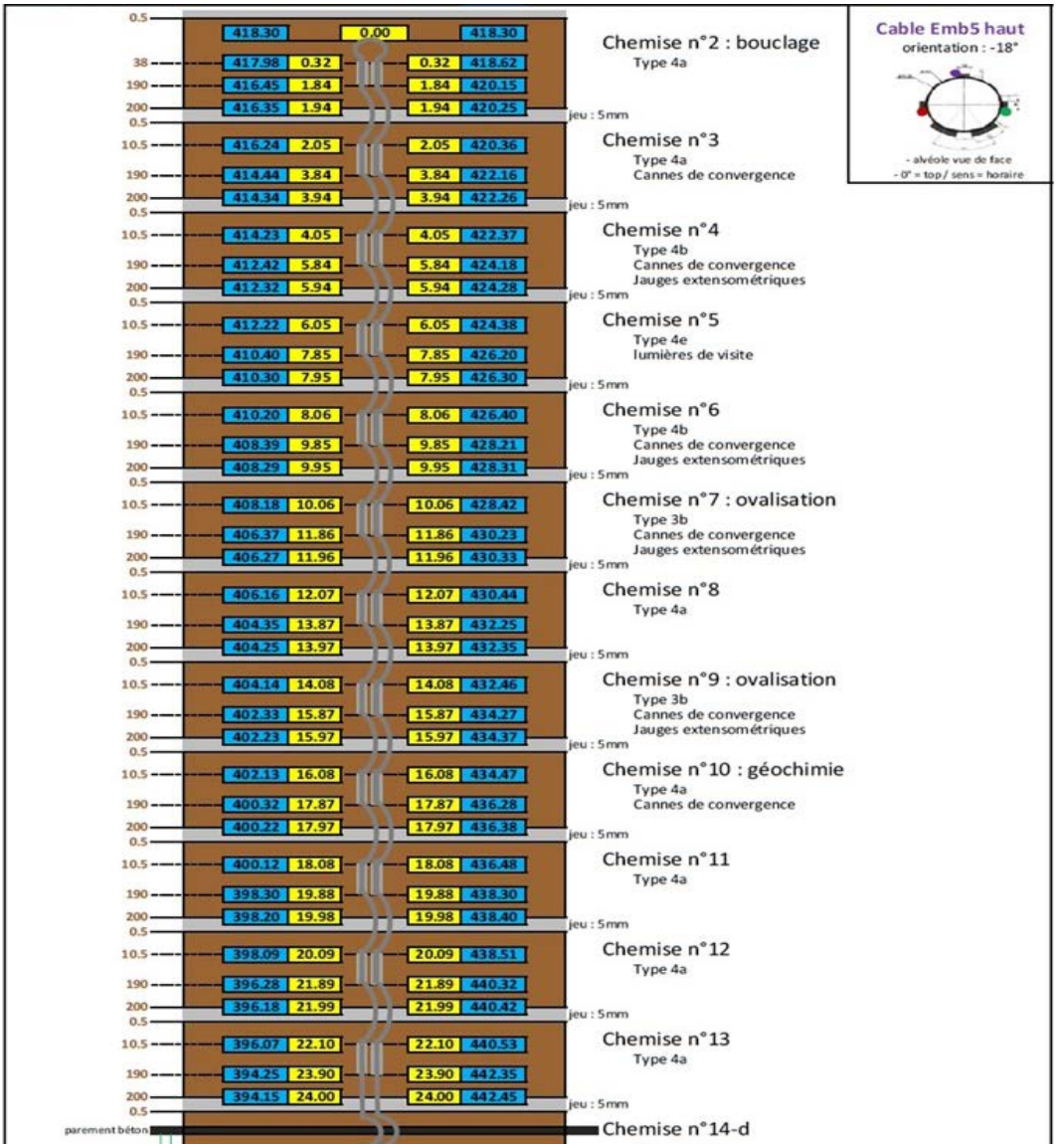

Figure 46: Emboss cable FN-SIL-05 TOP – layout after installation

5.5.1.2 Instrumentation of reference measurements

In order to assess, *in situ*, distributed OFS measurements several techniques were installed for both strains and temperatures. For instance, for OFS temperature measurements, it is well known that loss on the optical fiber induces shift on temperature measurements. In order to correct this shift, a classical platinum probes are often installed along the OFS cables in order to provide accurate temperature in well-known location. Then, it is easy to correct temperature shifts, along the OFS line, due to the losses, with just one reference measurement point for each optical line. More precisely, the probe can provide the expected correction if the optical line, between the probe and the end of the sensing OFS cable, does not contain any splice or connection (connector).

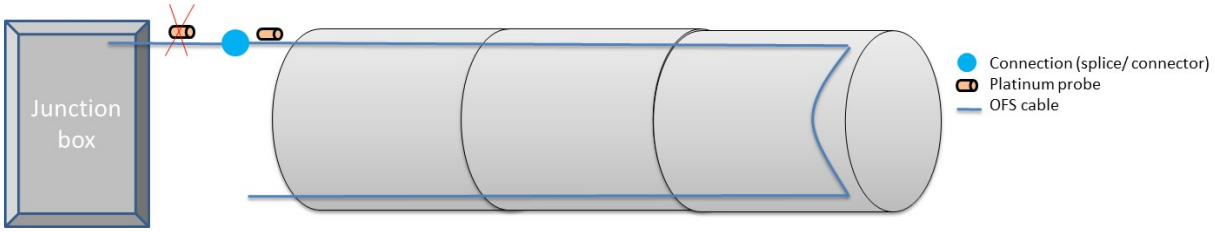

Figure 47: Illustration of the position of temperature probe along OFS cable to provide correct reference measurement for Raman scattering technique

5.5.1.3 OFS acquisition configuration

5.5.1.3.1 Fiber optic lines connection scheme

The sensing system was composed of several optical lines, as it has been done for AHA1604, where sensing parts are in the alveoli and optical interrogators are in G10 gallery).

5.5.1.3.2 Fiber optic connection scheme

The Neubrex interrogator has been connected to OFS cables according the following:

- Channel 6: Brugg cable V9 placed at the right orientation of the casing ;
- Channel 7: Neubrex cable Emboss-V5 placed at the left and (connected in series) up orientations of the casing ;
- Channel 8: Neubrex cable Emboss-V5 placed in spiral for ovalization measurement at sleeve 9 and (connected in series) sleeve 7.

The Silixa interrogator has been connected to OFS cables according the following:

- Channel 2 : Brugg cable T85 placed at the right orientation at the casing ;
- Channel 3 : Neubrex cable Emboss-V5 placed at the left connected to the up orientation at the casing ;
- Channel 4 : Neubrex cable Emboss-V5 placed in spiral for ovalization measurement at sleeve 7 and (connected in series) sleeve 9.

The Figure 48 presents the connection scheme for the lines *in situ* with each type of connection between fibers.

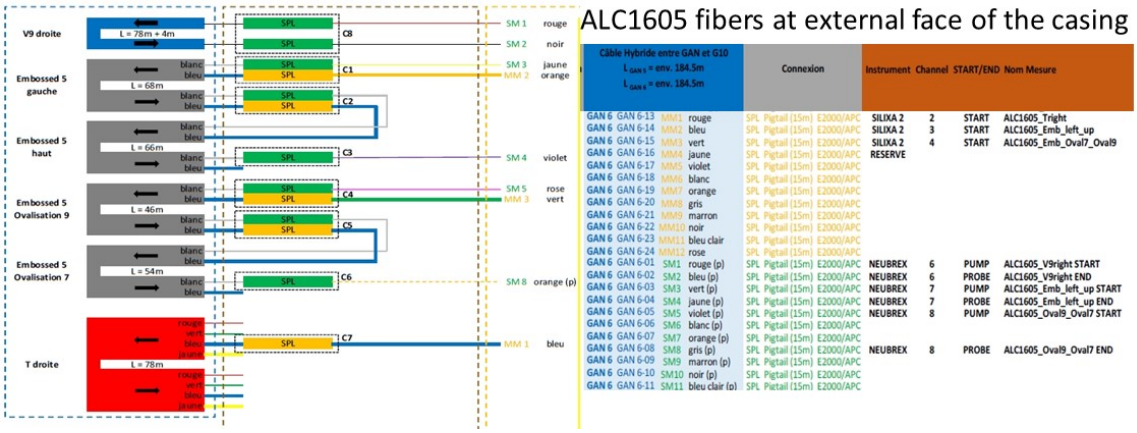

Câble Hybride entre GAN et G10			Connexion	Instrument	Channel	START/END	Nom Mesure
GAN 6 GAN 6-13	MM1	rouge	SPL Pigtail (15m) E2000/APC	SILIXA 2	2	START	ALC1605_Tright
GAN 6 GAN 6-14	MM2	bleu	SPL Pigtail (15m) E2000/APC	SILIXA 2	3	START	ALC1605_Emb_left_up
GAN 6 GAN 6-15	MM3	vert	SPL Pigtail (15m) E2000/APC	SILIXA 2	4	START	ALC1605_Emb_Oval7_Oval9
GAN 6 GAN 6-16	MM4	jaune	SPL Pigtail (15m) E2000/APC	RESERVE			
GAN 6 GAN 6-17	MM5	violet	SPL Pigtail (15m) E2000/APC				
GAN 6 GAN 6-18	MM6	blanc	SPL Pigtail (15m) E2000/APC				
GAN 6 GAN 6-19	MM7	orange	SPL Pigtail (15m) E2000/APC				
GAN 6 GAN 6-20	MM8	gris	SPL Pigtail (15m) E2000/APC				
GAN 6 GAN 6-21	MM9	marron	SPL Pigtail (15m) E2000/APC				
GAN 6 GAN 6-22	MM10	noir	SPL Pigtail (15m) E2000/APC				
GAN 6 GAN 6-23	MM11	bleu clair	SPL Pigtail (15m) E2000/APC				
GAN 6 GAN 6-24	MM12	rose	SPL Pigtail (15m) E2000/APC				
GAN 6 GAN 6-01	SM1	rouge (p)	SPL Pigtail (15m) E2000/APC	NEUBREX	6	PUMP	ALC1605_V9right START
GAN 6 GAN 6-02	SM2	bleu (p)	SPL Pigtail (15m) E2000/APC	NEUBREX	6	PROBE	ALC1605_V9right END
GAN 6 GAN 6-03	SM3	vert (p)	SPL Pigtail (15m) E2000/APC	NEUBREX	7	PUMP	ALC1605_Emb_left_up START
GAN 6 GAN 6-04	SM4	jaune (p)	SPL Pigtail (15m) E2000/APC	NEUBREX	7	PROBE	ALC1605_Emb_left_up END
GAN 6 GAN 6-05	SM5	violet (p)	SPL Pigtail (15m) E2000/APC	NEUBREX	8	PUMP	ALC1605_Oval9_Oval7 START
GAN 6 GAN 6-06	SM6	blanc (p)	SPL Pigtail (15m) E2000/APC				
GAN 6 GAN 6-07	SM7	orange (p)	SPL Pigtail (15m) E2000/APC				
GAN 6 GAN 6-08	SM8	gris (p)	SPL Pigtail (15m) E2000/APC	NEUBREX	8	PROBE	ALC1605_Oval9_Oval7 END
GAN 6 GAN 6-09	SM9	marron (p)	SPL Pigtail (15m) E2000/APC				
GAN 6 GAN 6-10	SM10	noir (p)	SPL Pigtail (15m) E2000/APC				
GAN 6 GAN 6-11	SM11	bleu clair (p)	SPL Pigtail (15m) E2000/APC				

Figure 48: Optical fibers and switch connection scheme to Neubrex and Silixa interrogators

5.5.1.4 Data acquisition

Unlike for AHA1604, OFS cables hasn't been monitored during installation process, but for grout injection of the cement material in the gap between the host rock and the casing all optical

lines were connected and monitored. Thanks to the test performed during injection of grout in AHA1604 demonstrator, the acquisition for ALC1605 injection was much more efficient. It has been monitored used the TW-COTDR method to capture the strain distribution. Then configuration has been modified for long term monitoring. All these configurations are listed, for one channel in Table 5.

Table 4 hardware settings during grout injection and for long term monitoring

example of channel 6	**Injection**		**Long term**	
Parameter	PPP	TW-COTDR	PPP	TW-COTDR
Distance range [m]	-	800	800	800
Spatial resolution [cm]	-	10	10	10
Sampling interval [cm]	-	5	5	5
Average count [-]	-	2^{10}	2^{15}	2^{13}
Pump output power [dBm]	-	0	0	0
Probe output power [dBm]	-	+29	+28	+28
Frequency start [GHz]	-	194150	10.25	194000
Frequency step [MHz]	-	200.0	2.0	200.0
Frequency count [-]	-	501	401	2001
Frequency end [GHz]	-	194250	11.05	194400

5.5.2 Temperature measurement by Pt100

These measurements allow a redundancy of the optical fiber for temperature measurement.

The sleeve n ° 7 is equipped with a section of 4 sensors type PT1000, located at 0 ° (top), 90 ° (right), 180 ° and 270 °, this on the same section of the jacket at 800mm from back end of the shirt. The sensors is glued on the liner, this under the protections of the spiral fiber, and the cables is brought on the same section to the two channels protected by protective covers: two cables (sensor 270 ° and 0 °) is thus brought to the high channel, and two (90 ° and 180 ° sensor) to the right channel.

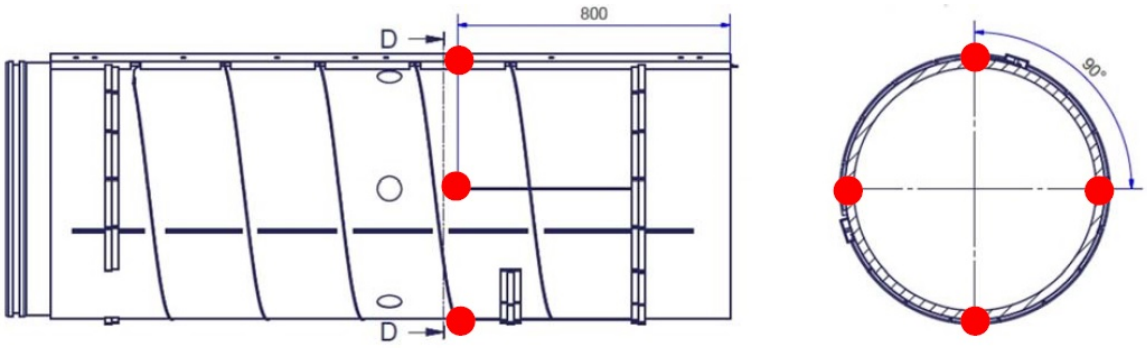

Figure 49: Sleeve n° 7: monitoring temperature section with4 PT1000 sensors

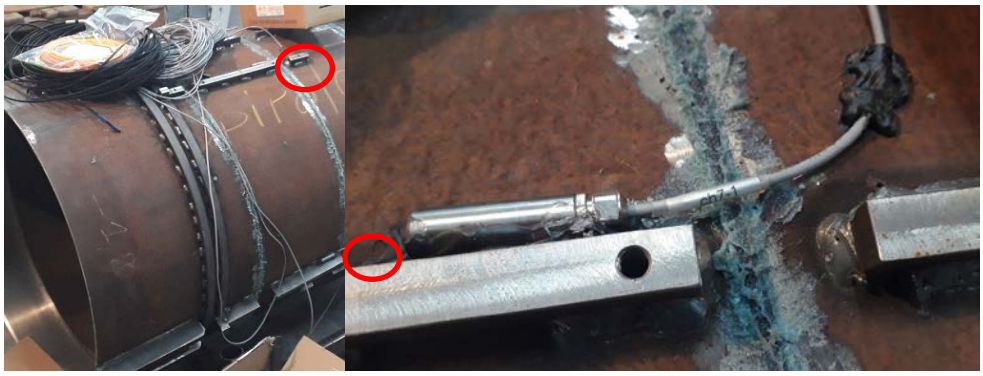

Figure 50 : picture of the Sleeve n°7 with Pt1000 sensors

5.5.3 Strain and ovalization measurement by vibrating wire

The sleeve n ° 9 was equipped with a section of 8 vibrating ropes type Geokon 4150 (see Figure 45) under the protection of the spiral fiber for the measurement of deformation and temperature, located on the same section at 0 ° (at the top), 45 °, 90 °, 135 °, 180 °, 225 °, 270 ° and 315 °, this to 1201.5mm of the back end of the shirt. The cables were brought on the same section to the two channels protected by protective covers: four cables (sensor 225 °, 270 °, 315 ° and 0 °) have thus brought to the high channel, and two (45 ° sensor). , 90 °, 135 ° and 180 °) to the right channel.

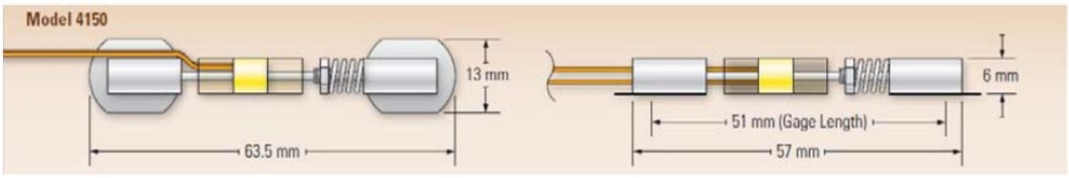

Figure 51: Geokon Vibrating wire 4150

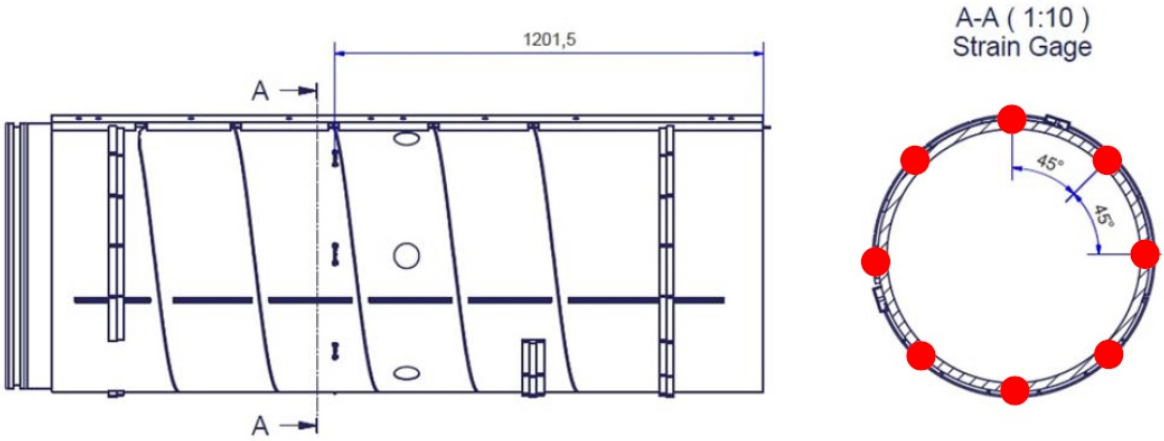

Figure 52 : identification of the position of vibrating wire sensor on the sleeve n°9

Figure 53 : Picture of the Geokong vibrating wire sensor 4150 on the sleeve before the installation of the protection system

5.5.4 Chemical instrumentation description

The monitoring of chemical parameters is very important in Cigéo and stands to safety issues. First, hydrogen realise and oxygen consumption are expected in the early age of the disposal alveoli. In addition of gas conditions, corrosion is expected to be slow and need to be assessed directly and indirectly (*via* parameters which affect the corrosion kinetic).

In order to measure these parameters, without maintenance or human intervention, Andra develops several technics and in this demonstrator, several were tested. All chemical sensors were installed at the external face of tube 10 (Figure 54).

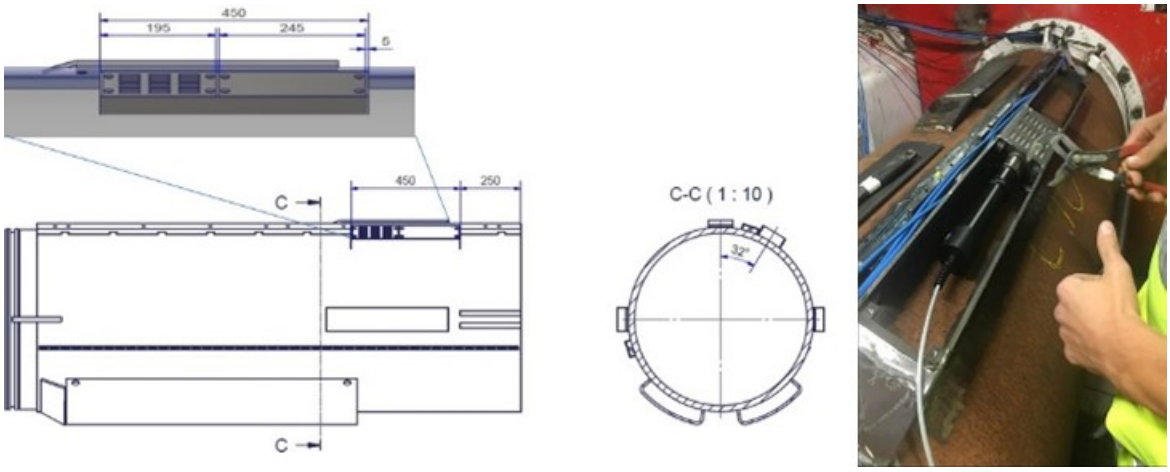

Figure 54: Scheme of the tube number 10 equipped with a chamber dedicated to collect water from the surrounding area and connection of sensors and fluid collecting tubes

This instrumentation consists of a chamber equipped with a porous sinter dedicated to stop cement grout material penetration and allowing only water to penetrate. This chamber has been connected to hydrogen sensor (thermal conductivity technique), dissolved oxygen sensor (electroluminescence technique) and fluid collecting tubs (2 for circulation allowance).

The tubes for fluid collecting will run to the gallery where they will be later connected to a modulus dedicated to water analyses. Two approaches are envisaged, in line analyses with analyser installed *in situ* and by collecting samples to be sent to laboratory for chemical analyses, both periodically. Sensors installed are listed below:

- Hamilton type VisiFerm 120 DO for O2 dissolved in water ;
- Developed sensor by Neroxis and Andra, based on thermal conductivity, for:
  - H2 ;
  - relative humidity ;
  - gas pressure ;
- Platinum probe type PT1000 for thermal affect assessment.

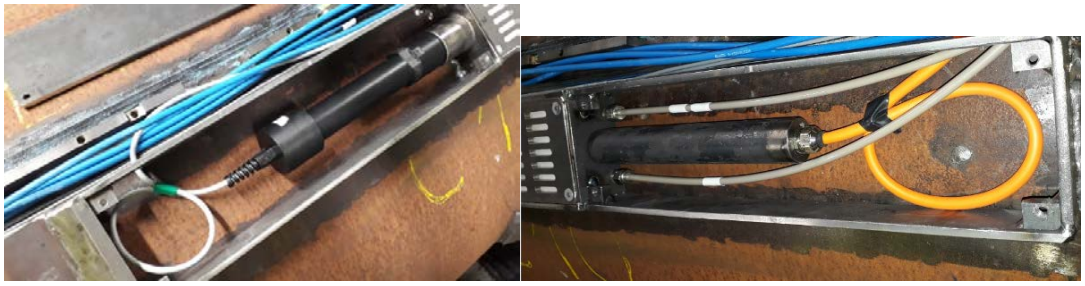

Figure 55: Some picture of the instalaltion of the H2 et O2 sensors on the sleeves n°10 with Peek lines for future comparative measurement

5.6 Measurements results on ALC1605 demonstrator

The first results obtained *in situ* were analysed for several purposes. During grout injection in the gap between casing and the surrounding rock phase data was intended to help assessing filling's quality. Also thermos-mechanical evolution of the casing will be monitored, before, during et after heating of the casing. The long term monitoring will validate ovalization assessment, longitudinal strain and temperature measurements, installation method and robustness for all optical lines.

5.6.1 Strain distribution during grout injection

The construction process for ALC1605 is the same of AHA1604. Although, grout injection has been monitored in order to assess filling quality. Obtained raw data indicate clear observation of the changes according to the grout front arrival along the casing. Figure 34 indicates for each casing element, colored, the corresponding evolution on the curves with same color.

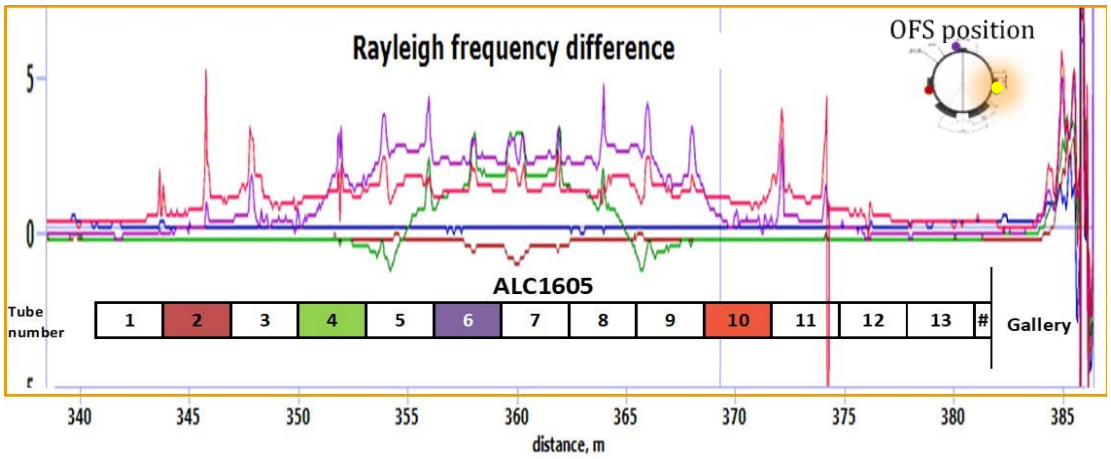

Figure 56: Rayleigh frequency changes during injection phase observed by OFS cable at the top right position (bright yellow circle along the casing at several localization.

Data obtained on platinum probes and vibrating wire extensometers were acquired in order to compare data to those obtained by distributed OFS cables. The Figure 51 shows the results obtained.

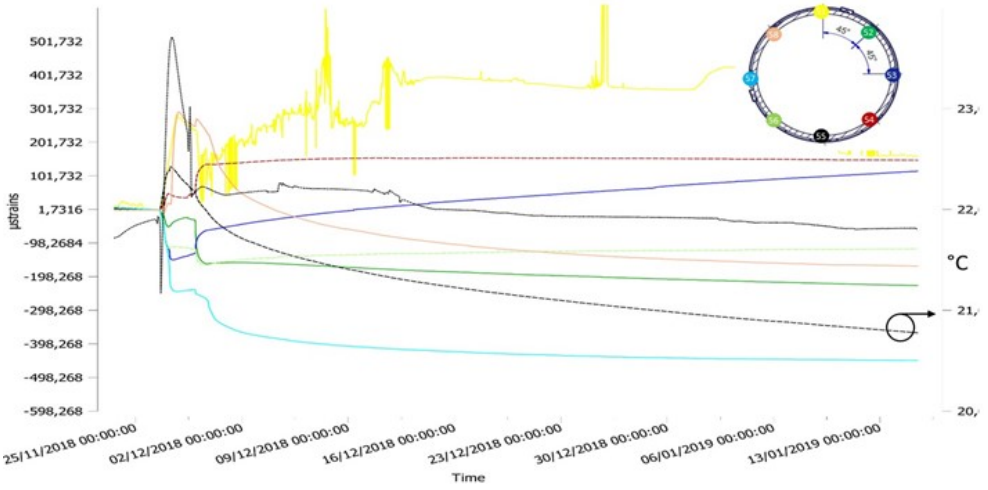

Figure 57 : Strains measured by extensometers at the external surface of the casing, tube 7 in redundancy of spiraled OFS and temperatures measured by platinum probe

Temperatures were measured around tube 7 and 9, both equipped with spiraled OFS cable. The tube 9 was equipped (see. Figure 31) with four platinum probes, and tube 7 was equipped with 8 VWE (see. Figure 32) which deliver strains and, via thermistors, temperatures.

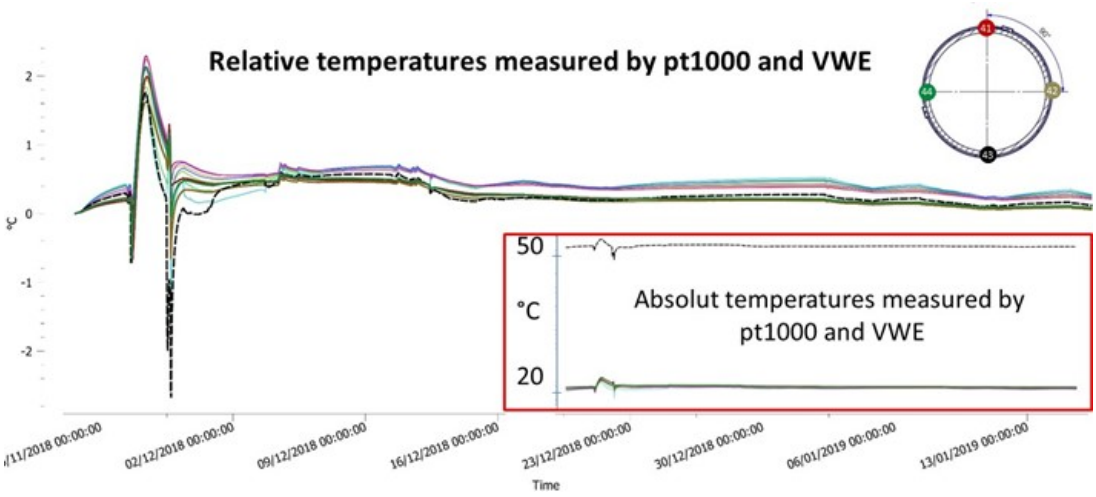

Figure 58: Temperatures measured by classical sensors (platinum probes and thermistor placed in the VWE) at tubes 7 and 9, relative temperatures and in corner absolute temperatures

One can see in Figure 36 that one of the sensors provide temperatures with an offset (about 30°C). Relative measurements shows that temperature changes fit well, in term of values and behavior with all the other temperature sensors.

6 Summary, conclusion and future works

The Cigeo monitoring plan that describe processes and parameter to be monitored should proposes an instrumentation to be used for monitoring the HLW cell and give design example based on full scale experiment done in the underground facility.

Inside the "AHA program" dedicated to the evaluation of the technical feasibility of cell construction and performance assessment, monitoring aspects are included as part of the evaluation. Monitoring parameters determination were found based on the analyse on the long term safety and reversibility requirement. Andra develop a method based on the analyse of process (PARS) to select parameters. The screening methodology was also used to consolidate the parameters selection. Monitoring parameters selection was not explain in the present document (*Modern2020 D2.2*).

The monitoring design for the HLW cell has been elaborated based on process knowledge collect in the URL of MHM, the maturity of monitoring technology and construction constrain.

A stepwise procedure has been elaborated to gradually consolidate the monitoring design, implementation method and sensor performance. In this way, Three HLW prototypes structure inside the "AHA program" were used to evaluate monitoring system: AHA1604 (Nov. 2017), ALC1605 (Nov. 2018) and AHA1605 (plan to be realize in July 2019). Experiment is conducted from a light (AHA1604) to heavy instrumented (AHA1605) test set up.

Only the two first experiment has been shown in this report.

6.1 AHA 1604 Summary and recommendation

The main outcome of the AHA1604 experiment was the demonstration of the capability to build HLW cell with a length superior to 100m. The depth of 112.5 m has been achieve demonstrate that it is possible to excavate micro-tunnel and to emplace the metallic casing and ground material using the new HLW concept.

Application of distributed optical fiber-optic to monitor temperature and strain was used for the first time with the new HLW concept. The conventional Raman DTS was used to monitor temperature during the different phase of the demonstrator. In the same time Brillouin and Rayleigh measurement were performed to measure strain. The measurements were based on knowledge prior to the installation, which were very limited. The overall measurements quality is good

The experimental setting was elaborated also to evaluate method to laying OFS on metallic liner (glue or anchor point).

As summarized below, the preliminary results showed positive insights for measuring temperature and strain even if more effort should done for the data treatment

Recommendation

Optical budget of the measuring line:

the overall measurements quality is good, however, the increase in laser optical power (both probe and pump side) resulted in failed calibration adjustment procedure for some of the measurements. As a consequence, these measurements might have a constant offset along the fiber. This has been corrected and improvements were expected for the next installation.

Improvement of the accuracy during injection phase:

The measurements during grout injection were performed only on channel 1 (V9 left), using Brillouin based sensing, using the same measurement settings as during installation stage. The measurement method as well as shields, protecting the OFS, made difficult the grout front

movement detection. Despite there is clearly visible injection start event, the actual grout front is difficult to determine.

Also, the measurements should better be performed on the helically installed OFS, as it could provide on grout distribution and uniformity. **t**he recommendations to improve next installation monitoring were:

- In order to detect movement of the grout, the Rayleigh measurements must be used ; Brillouin type measurements should be changes to Rayleigh-based ;
- For Rayleigh measurements, to reduce measurement time, the frequency range should be adjusted to make it as narrow as possible ;
- To obtain better spatial resolution, Embossed cable should be measured (as it is installed in a spiral pattern) ;
- For calculating frequency shifts, the previous measurement should be used as reference.

Strain distribution

The strain distribution within glued segments of channel 1 fiber (segments K-L, M-N, O-P, and R-S) are quasi uniform, and are within 100 με range. This indicates that the installation process was performed correctly and proper pre-tension was used. However, once the grout injection started the strain distribution in the same segments becomes considerably less uniform.

A shift on Cartesian coordinate system used-

The measurements indicated small differences between mapped coordinates, provided by the company in charge of the installation, and the key locations measured by the instrument along the OFS cable. This difference is negligible and has no effect, except a shift on localizations, along the OFS cable. During installation process, it was determined that the offset due to additional connection cables used, was 55.53 m.

Permanently installed OFS cables also indicated small differences, all within 15 cm, between reported and observed locations. These differences, however, should be considered as typical during such a complex installation. In general, there is a good match between received cable layouts and observed locations on data.

Long-base fiber extensometers

The fiber on channel 1 was glued at 4 points across 4 Tube elements. This created the segments of uniform strain and 3 virtual extensometers. The installed strain varied between respective segments as was higher by 10,000 με, 4,000 με, and 1,000 με respectively. This indicates that the Tubes (components) might be misaligned. This is very important engineering indicator, and should be taken into account in subsequent installations.

Thermal strain due to cement curing

The measurements during installation and grout injection phases were performed using Brillouin backscattering based sensing. This means that strain-temperature separation was not performed and there is no pure temperature data available, while the fibers are subject to high strain changes. However, once the injection process completed, the strain changes should be mainly due to the grout/concrete curing and considered mainly as thermal strain. The gradual increase in strain value in time is clearly visible.

6.2 ALC1605 Summary and recommendation

The phase 1 of ALC1605 experiment has been successfully performed. This step include the construction of the demonstrator and the implementation of the monitoring system. The phase 2 include the installation of the heating system and the ignition.

The installation of OFS cables and redundant sensors, for ALC1605 demonstrator, succeeded thanks to feedback obtained on AHA1604 installation.

6.2.1 Grout movement

Coordinate mapping

The measurements indicated small differences between mapped coordinates received from Solexperts and key locations measured along the fiber. Permanently installed fiber cables also indicated small differences, all within 10-15 cm, between reported and actual locations. These differences, however, should be considered as very typical during such a complex installation.

In general, there is a good match between received cable layouts and actual data/locations.

Grout movement

The measurements during grout injection were performed solely using Rayleigh based sensing. The measurement method as well as shields protecting the fiber made the grout front movement detection difficult but possible. Despite there is clearly visible injection start event, and grout front can be relatively easily determined. The values of induced strain at initial part of the injection operation is around 30 to 50 micro-epsilon or less. This clearly explains why the monitoring for AHA 1604 with Brillouin based sensing did not provide reliable measurements data. With Rayleigh based sensing that improved substantially and glued portion of the cable provide accurate data.

Thermal strain due to cement curing

The measurements during installation and grout injection phases were performed using Rayleigh backscattering based sensing. This means that strain-temperature separation was not performed and there is no pure temperature data available, while the fibers are subject to strain changes. However, once the injection process completed, the strain changes should be mainly due to the grout/concrete curing and considered mainly as thermal strain. The gradual increase in strain value in time would be clearly visible in trend plots. However, the measurements were stopped far too early to properly detect data. The detailed analysis of long term monitoring data might provide that information.

6.2.2 Sensors implementation

Pt1000

One sensors failed for an undetermined reason, investigation are in progress

vibrating wire section

One sensors provide inconsistent data, investigation are also in progress.

OFS sensors

100% of OFS sensor are operating. Progress has been made been the AHA1604 demonstrator to follow the filling material injection

6.3 Future works (AHA1605)

The AHA1605 alveolus will be excavated, in GAN gallery in Andra's URL (Figure 20), mid 2019. This demonstrator aims to validate HWL monitoring concept. It will be the achievement of several tests performed at previous demonstrators (AHA1604, ALC1605).

The objective are:

Set a complete monitoring system on HLW type structure covering the monitoring parameters selected

Set evidence on the monitoring system in support to the licence application process

- Demonstrate Andra's ability to instrument a 80m centered cell;
- Optimize instrumentation by testing several installation configurations and different technologies;
- Initiate the Acceptance test through robotic measurement

• Validate measurements performance: calibration, maintenance, frequency of measurements, ...

The envisaged drilled depth of the AHA1605 alveolus is 82.5 m, in order to have 80 m of casing in the borehole, as planned in Cigéo. The construction bill be similar to ALC1605 concept, with casing and grouting material in the gap between the casing and the surrounding rock.

Figure 59 presents the distribution of the sensors, planned to be install, at external surface of the casing, internal surface and inside the casing.

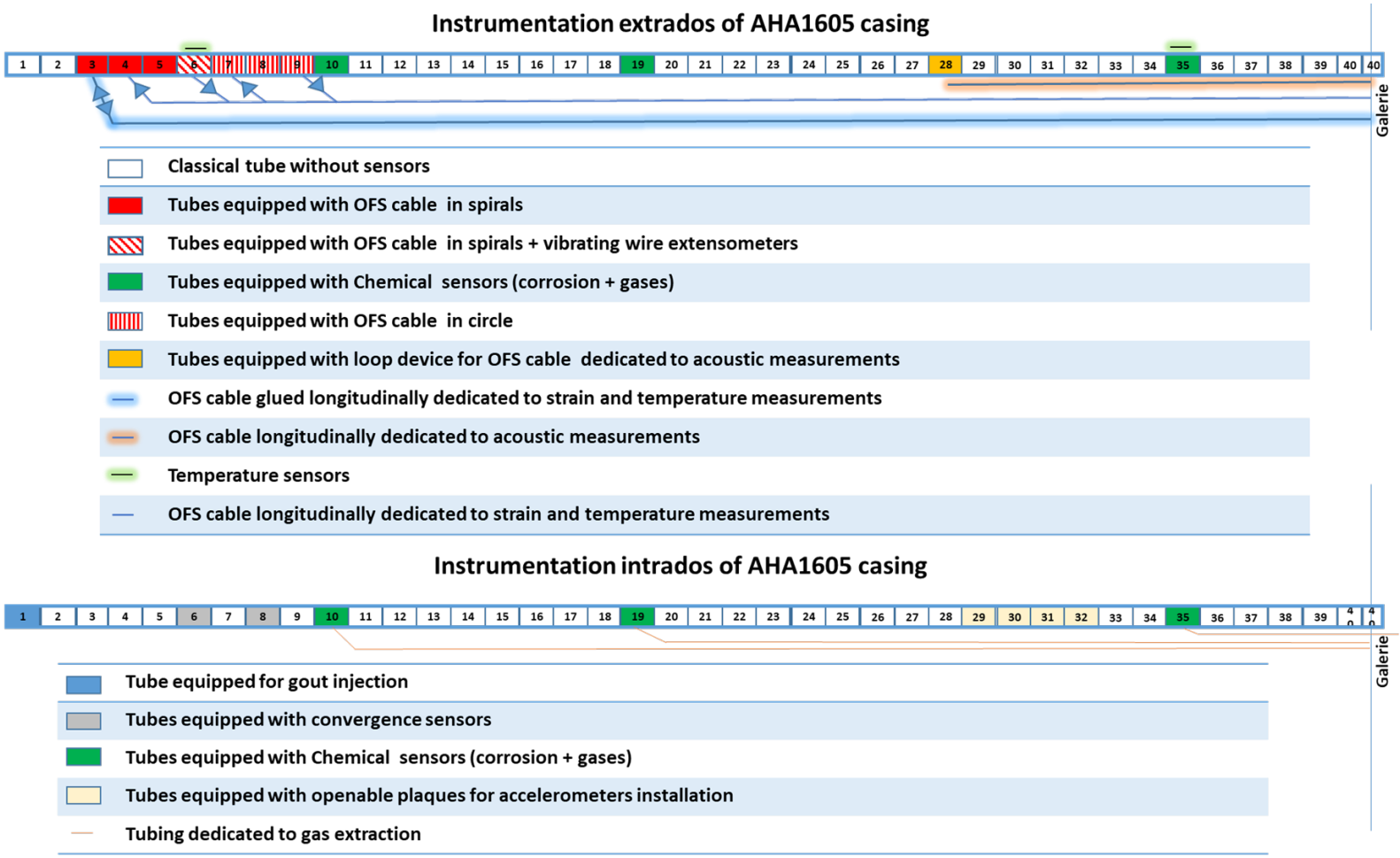

Figure 59: Drawing of the monitoring system evaluate on the AHA1605 cell

Principal evolution for the AHA1605 monitoring system

Near field monitoring system

The instrumentation at the periphery of the AHA1605 cell meets the following objectives:

- In the short term: evaluate geophysical techniques (acoustic and electrical) to characterize the damaged area without sampling and without human intervention (after installation), ie compatible with use in Cigéo;
- In the longer term: to qualify techniques allowing to follow the evolution of the damaged zone (extension and properties) during the life of the storage.

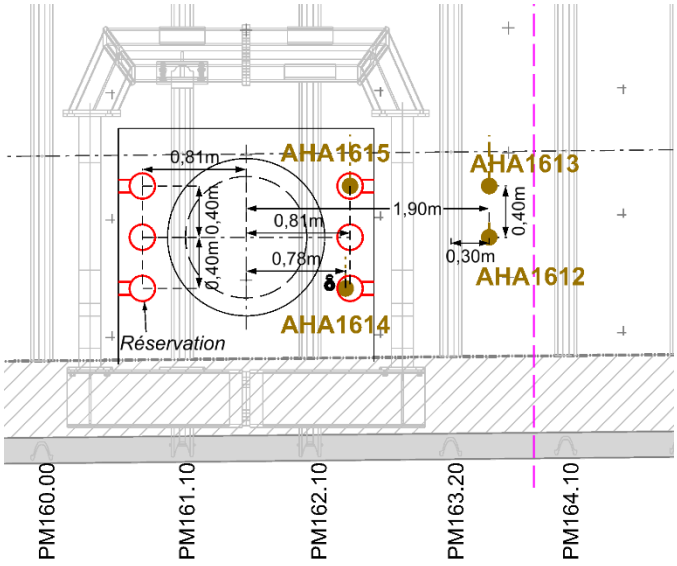

Figure 60: localisation of the monitoring borehole in the surrounding of the AHA1605 cell

Robotic measurement system

The purpose of this system is to obtain measurements for validating other previously-installed monitoring systems

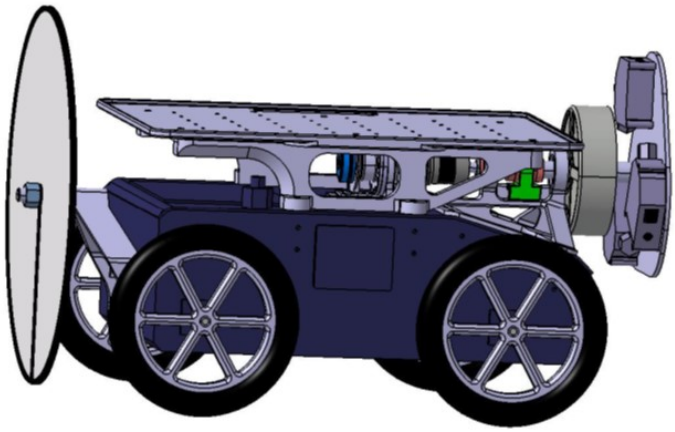

Figure 61: SAM robot

Corrosion measurement

Evaluation of corrosion measurement system will be done on different region of the AHA1605 cell. Three technique will be evaluated

- Aircorr® solution which is asystem for continuous monitoring of atmospheric corrosivity. An electronic unit measures and records changes in the electrical resistance of a thin metal track applied on an insulating substrate.
- Electrochemical probe
- Corrosion coupon (reference solution): design and sampling method will be evaluate

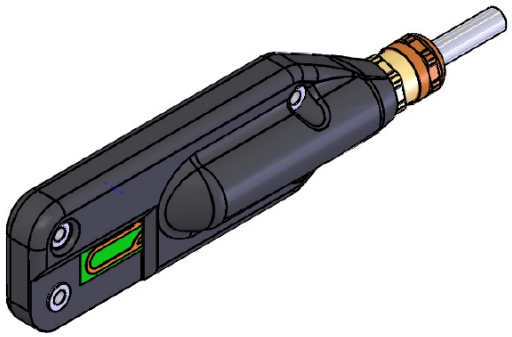

Figure 62: Aicorr sensor developed for the corrosion monitoring

Geochemical measurement

Evaluation of the gas and liquid will be done at the external and internal of the AHA1605.

- Direct measurement of the gas phase will be done by H2 and O2 sensors
- Water sampling will be perform and analyse by system in the GAN gallery

Further optimization on optical fibers

Strain and temperature using optical fiber will be used in way to simplify the design. A example could be see on Figure 63 for the measurement on ovalization where the number of cable spire is reduced as only 2 b-circle line. Comparison with old system will be compare to the new one. A new generation of optical fiber cable will be used also.

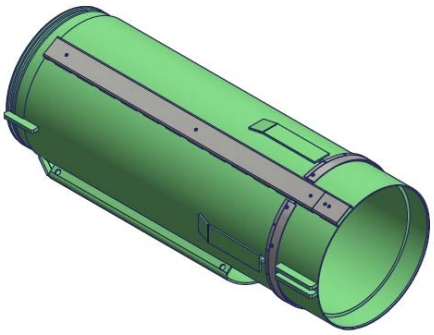

Figure 63: Bi-circle configuration for ovalization measurement using optical fiber sensors

7 References

[1].R. Farhoud et al., Monitoring system design of underground repository for radioactive wastes – in situ demonstrator, International Journal of Engineering and Technology, 7, 6, 484-489.

[2].A. Rogers et al., 1999. Distributed optical fiber sensing, Measurement Science Technology, pp. 75-99, 1999.

[3].Y. Yamauchi et al., A measurement method to determine strain and temperature coefficients in fiber optic sensors, Proceedings of Asia-Pacific Workshop on Structural Health Monitoring, Tokyo, 2010.

[4].K. Kishida et al., Study of Optical Fibers Strain-Temperature Sensitivities Using Hybrid Brillouin-Rayleigh System, Photonic Sensors, 10, 1007, 13320-013-0136-1.

[5].F. Bumbieler, S. Necib, J. Morel, D. Crusset, G. Armand Mechanical and SCC behaviour of an API5L steel casing within the context of the deep geological repositories for radioactive waste, Proceedings of the 2015 ASME Pressure Vessels & Piping Conference, PVP2015, Boston, Massachusetts, USA (2015)

[6].Cementitious slurry for filling an annular space around a radioactive waste repository galery excavated in a clay medium Ref. FR3031103(A1)

[7].deliverable (D-N°:D3:04) Final Report LUCOEX – WP3

8 Appendix:

8.1 A 1: Technical specifications of the optical fiber cables

NEUBREX

FutureNeuro™ FN-SILL-3

Embossed Sensing Cable

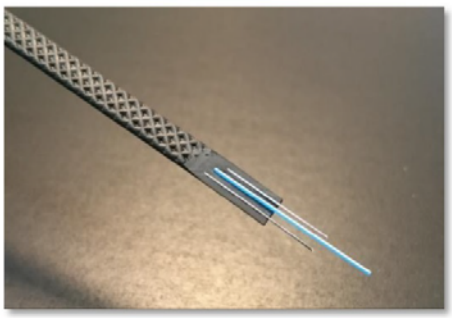

FEATURES

- Two Sensing Fibers
- Long-term Heat Resistance up to 80 °C
- Tensile Strength holds up to 25kg-f
- Without Elastic Hysteresis Effects
- Non-slippery Embossed Sheath

The FN-SILL-3 is sensing fiber cable for Strain and Temperature measurement. Two sensing fibers are set side by side in the center of cable. And two strength members are set paralleled along with sensing fibers, for holding up to 7.5kg force tensile strength. With its embossed grid on the sheath that make it easily embedded into or stuck onto the measure object.

The outer sheath is made from Olefinic Elastomers, which has superior character of no elastic hysteresis, long-term heat resistance, and UV-resistance. Thus, FN-SILL-3 ensures the linear responses that transferred from the object, either strain or temperature measurement.

Thermal Cycle Tests

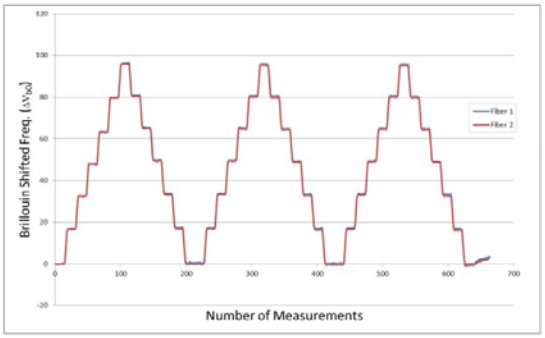

The pictures in left shows the FN-SILL-3 had a 40hrs cycle tests in 「20-80-20°C, step 10°C」 pattern in chamber, and gathered 640,000+ data for hysteresis effects analysis. The lines represent those 2 fibers in the cable.

The result denotes the cable maintained its structure well during the tests. As recognized, the strength members keep its low elongation and deformation characters during temperature changing.

Application Sample

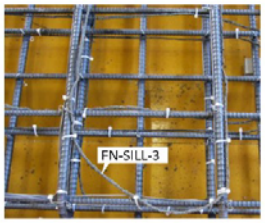

The picture shows in the left that denotes how the FN-SILL-3 embedded with Reinforced Concrete structure. The sensing fiber ties together with rebar for strain measurement.

In this picture, the FN-SILL-3 has pre-soaked with cement mortar for quickly adapting to premixed concrete in this experiment. Ordinary, FN-SILL-3 does not necessary to pre-soaked with cement due to it's embossed sheath.

Rev. 3.0 12/2016

NEUBREX

FutureNeuro™ FN-SILL-3

Embossed Sensing Cable

SPECIFICATIONS

Fiber Type	10 / 125 μm Single-mode Fiber
Fiber Count	2
Attenuation	< 0.5 dB/km
Strain Sensing Range* (Δε)	5000 με
Temperature Sensing Range	-20 to +80 °C
Bending Radius	> 40 mm
Strength Member	ϕ0.3mm, SUS304 x2
Tensile Strength	25 kg-f
Dimension (W x H)	4.3 x 1.7 mm
Max. Delivery Length	2000 m
Weight	12 g /m
Operation Temperature	-20 to +80 °C
Storage Temperature	-40 to +85 °C

* Will depending on the real applying situation of the cable. Please contact us for more information.
** All specifications above are subject to change without notice.

CONFIGURATIONS

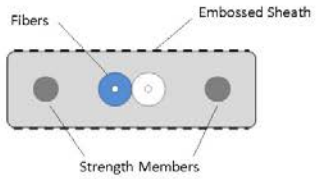

DELIVERY REEL +

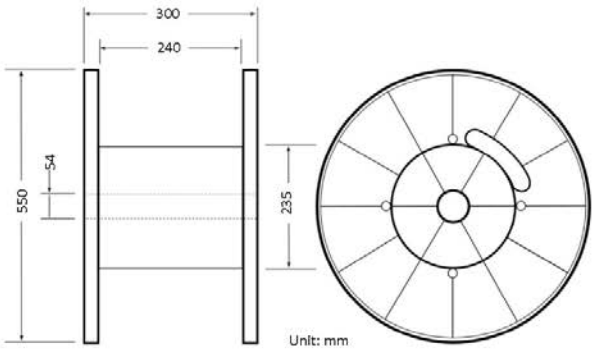

+ Delivery reel could be various per different cable length and customer requirement.

NEUBREX
Neubrex Co., Ltd.
Sakaemachi-dori 1-1-24, Chuo-ku, Kobe
Hyogo 650-0023, Japan
Tel: +81-78-335-3510
www.neubrex.com

Fibre Optic Sensing Cable

BRUsens Temperature 85°C

3_50_1.025

LLK-BSTE 85°C 4.8 mm

Small fiber optic metallic temperature sensing cable, armored with stainless steel loose tube, metal strength members and PA outer sheath, fast thermal response, for up to 4 fibers

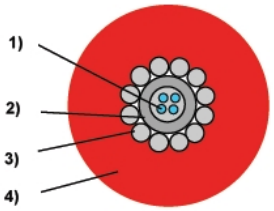

Construction:
- 1) Fibers with dual layer acrylate coating for increased micro bending performance
- 2) Gel-filled stainless steel 316L, metal loose tube
- 3) Stainless steel wires, 316L
- 4) PA outer sheath

Description:
- Central metal loose tube with up to 4 fibers, hermetically sealed
- High tensile strength
- High crush resistance
- Longitudinally and laterally watertight
- High chemical resistance
- Robust cable sheath
- Excellent rodent protection
- Compact design, high flexibility

Applications:
- Subsea monitoring of high voltage power cables
- Temperature monitoring
- Sensing applications, Raman
- Harsh environment, outdoors, indoors
- Deployment in conduits or directly in the ground

Standard optical fiber:
- Single-mode fiber: ITU-T G.652.D
- Multimode fiber 50/125 OM2
- Other fiber types and fiber quality available upon request

Temperature range:
- Operating temperature: -40° C ... +85° C
- Storage temperature: -40° C ... +85° C
- Installation temperature: -10° C ... +50° C

Cable sheath color:
- Red, similar RAL 3000
- Other colors upon request

Standards:
- Cable tests complying with IEC 60794-1-2

Remarks:
- Fiber color code to be agreed
- Other cable designs and temperature ranges available
- Standard cable marking with meter marks, special labeling of outer sheath upon request
- Accessories such as loops, fan outs, connectors, mounting brackets etc. available
- Deployment training upon request
- For improved UV resistance, black cable sheath available upon request

Technical data:

Type	Max. no. of fibers	Cable ø	Weight	Max. tensile strength	
	units	mm	kg/km	installation N	operation N
4F	4	4.8	42	1300	900

Type	Min. bending radius		Max. crush resistance
	with tensile mm	without tensile mm	N/cm
4F	20xD	15xD	800

Optical fiber data (cabled) at 20°C

Fiber Type	Attenuation, dB/km			Modal Bandwidth, MHz·km	
	850 nm	1300 / 1310 nm	1550 nm	850 nm	1300 nm
MMF 50/125	≤ 3.0	≤ 1.0	NA	700	500
SMF	NA	≤ 0.36	≤ 0.22	NA	NA

Subject to changes without notice

2016/12/19/ Rev.03 TH

BRUGG CABLES Well connected.

FIBER OPTIC SYSTEMS
Brugg Kabel AG • Klosterzelgstrasse 28 • 5201 Brugg • Switzerland
Phone +41 56 460 3333 • info.fosy@brugg.com

Fibre Optic Sensing Cables

BRUsens strain V9

3_50_2_005

LLK-BSST V9 3.2 mm

Flexible, mini armored fiber optic strain sensing cable with central metal tube, structured PA outer sheath, one optical fiber, strain range up to 1% (10000 µstrain)

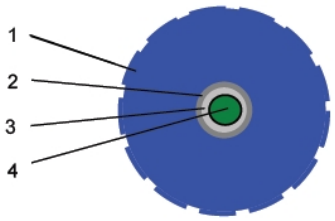

Construction:
- 1) PA outer sheath, with structured surface with interlocking system
- 2) Metal tube SS316L for protection and hermetic seal
- 3) Multi layer buffer and strain transfer layer with interlocking system
- 4) Special strain sensing optical single mode fiber

Description:
- Central metal tube with 1 optical fiber
- Good tensile strength
- Longitudinally and laterally watertight
- Good rodent protection
- High strain sensitivity
- Compact design, good flexibility, small bending radius
- Abrasion resistant structured sheath, for better strain transfer
- Halogen-free cable sheath

Applications:
- Distributed strain sensing
- Sensing technologies: Brillouin, FBG
- Precision measurement and alarm systems
- Soil movement, ground monitoring
- Pipeline monitoring
- Structural monitoring
- Direct burial in soil, concrete
- Harsh environment, subsea, outdoors

Standard optical fiber:
- Single-mode fiber: ITU-T G.657
- Other fiber types and fiber quality available upon request

Temperature range:
- Operating temperature: - 30° C ... +70° C
- Storage temperature: - 40° C ... +70° C
- Installation temperature: - 10° C ... +50° C
- Short term temperature (60 min) +150°C (during installation)

Cable sheath color:
- Blue, similar RAL 5005
- Other colors upon request

Standards:
- Cable tests complying with IEC 60794-1-2

Remarks:
- Fiber colored
- Final test reports OTDR and BOTDA measurement
- Other cable designs and temperature ranges available
- Standard cable marking with meter marks, special labeling of outer sheath upon request
- Preassembled cable sets available, special field termination kit available
- Accessories such as anchors, loops, fan-outs, splice enclosures, connectors, etc. available
- Deployment training upon request
- For improved UV resistance, black cable sheath available upon request

Technical data:

Type	Max. no. of fibres units	Cable ø mm	Weight kg/km	Max. tensile strength installation N	Typical Load at 1% elongation N
1F	1	3.2	10.5	260	470

Type	Min. bending radius		Max. crush resistance
	with tensile mm	without tensile mm	N/cm
1F	64 (20xD)	48 (15xD)	250

Optical fiber data (cabled) at 20°C

Fiber Type	Attenuation, dB/km	Typical Brillouin parameters BOTDR or BOTDA at 1550 nm		
	1550 nm	Temperature sensitivity df_B / dT	Strain sensitivity $df_B/d\varepsilon$	Centr. Brillouin Freq.
SMF	≤ 0.5	1.1 MHz/°C	450 MHz/%	10.6 GHz

2016/06/07 Rev. 02 TH

BRUGG CABLES Well connected.
SENSING TECHNOLOGIES
Brugg Kabel AG • Klosterzelgstrasse 28 • 5201 Brugg • Switzerland
Phone +41 56 460 3333 • info.sensing@brugg.com • www.bruggcables.com/sensing

8.2 A2: Technical specifications of Neubrescope instrument

NBX-7020-S system

Function	Property						
General Function	Separation of strain and temperature measured in single fiber PPP-BOTDA / BOTDR / TW-COTDR / COTDR						
Function	PPP-BOTDA (BOTDR)						TW-COT
Laser wavelength	1550±2 nm						1530 nr
Distance range	50 m, 100 m, 250 m, 500 m, 1 km, 2.5 km, 5 km, 10 km, 25 km						
Measurement frequency range	9~13 GHz						192300
Range of strain measurements	-30,000 to +40,000 με (-3% to +4%)						-15,000
Measurement frequency scan step	1, 2, 5, 10, 20, 50 MHz						100, 20(
Readout resolution	5 cm (default), 1cm (maximum)						
Sampling points	600,000 (default), 3,000,000 (maximum)						
Average count settings	$2^5 \sim 2^{23}$ times (including Hardware Average Count $2^5 \sim 2^{16}$)						
Pulse width, ns	0.2	0.5	1	2	5	10	0.2
Spatial resolution, cm	2	5	10	20	50	100	2
Dynamic range, dB *1	0.5	1	1.5	3	3.5 (1)	6 (2)	0.5
Max. measurement Distance, km *2	0.5	1	2	5	12 (3)	20 (6)	0.5
Optical budget, dB*1*8	1	2	5	7	10 (3)	12 (6)	1
Measurement accuracy *3*4	15 με/0.75 °C		7.5 με/0.35 °C		5 με / 0.25 °C		0.5 με /
Repeatability *3*4*5	10 με / 0.5°C		2.4 με / 0.1 °C		2 με / 0.1°C		0.2 με /
Measurement Accuracy of BOTDR *3*4	-			75 με/ 3.5°C	50με / 2.5°C	30 με/ 1.5°C	-
Repeatability of BOTDR *3*4*5	-			20 με / 1 °C			-
Measurement time *6*7	5 seconds (minimum)						60 seco
Measurement accuracy for hybrid mode *9	10 με / 0.5 °C						
Repeatability for hybrid mode *9	5 με / 0.25 °C						
Input-output fiber	Single mode optical fiber						
Fiber connector	FC-APC / SC-APC (factory option)						
Suitable fiber	Single mode optical fiber						
Power supply	AC 100~240V 50/60 Hz 250 VA						
Laser class	Class 1 (IEC60825-1 : 2001)						
Dimensions / Weight	approx. 456(W) × 485(D) ×286(H) mm / 30 kg						
Operating temperature	10 ~ 40 °C, Humidity below 85 % (no dew condensation)						
Storage temperature	0 ~ 50 °C						
Place of production	Japan						

*1 Based on 2^15 average cycles
*2 Based on average fiber loss of 0.3dB/km using SM fiber(UV type)
*3 Based on the measurement of strain free SM fiber(UV type)
*4 Based on the measurement of strain-free SM fiber(UV type) and in constant temperature environment
*5 The maximum deviation range of measurement value for 5 consecutive measurements for 100 consecutive points
*6 Within the setting of 50m range, 2^13 count settings, 41scan steps except the time of Pre-Pump Adjustment
*7 Within the setting of 50m range, 2^13 count settings, 401scan steps except the time of Pulse Output Adjustment
*8 Within the allowable range being adjusted by the optical power, except the case of nonlinear phenomena
*1-*5 are based on a frequency scan step of 5MHz when using PPP-BOTDA and with Pre-Pump Adjustment and Auto Frequency Adjustment on
*1-*5 are based on a frequency scan step of 250MHz by using TW COTDR and with Pre-Pump Adjustment and Auto Frequency Adjustment on

Appendix 2.1 Specification of accompanying computer

The instrument is controled from application installed and running on workstation Dell Precision Tower 5000 Series (5810). Its technical specifications are summarized in Table 7.

Table 5 Specifications of the Dell Precision Tower 5000 Series (5810) workstation

Function	Property
Operating System	Microsoft® Windows® 7 Professional
CPU	Intel® Xeon® Quad Core Processor
Memory	16 GB
HDD	1 TB
Display	21.5 inches
CD-ROM Drive	Installed
Ethernet Port	1 (1000BASE-T / 100BASE-TX / 10BASE-T)
USB Port	9
Keyboard	Dell KB216 Wired Keyboard English Black
Size (W x D x H)	Mid-Tower Chassis - 16.30 x 6.79 x 18.54"; 414 x 172.6 x 471mm
Power Supply	AC 100 V – 240 V (50/60 Hz)

Appendix 2.2 Optical switch

In order to provide continuous measurements of different optical fiber lines, the instrument was connected to optical switch NBX-1000-3 (2 x 8 x 2 = 16 x 2 channels).

Figure 64 NBX-1000-3 (8 x 2) optical switch - component

Table 6 Technical specifications of NBX-1000-3 optical switch

Item	Specifications
Durability	No wear out (no mechanical parts)
Suitable Optical Fiber	SM
Suitable Optical Connector	E2000
Wavelength range (nm)	1240~1640
Insertion loss (dB)	≤2.0 (typical 1.5)
Switching time (ms)	≤ 1 (typical 0.5)
Operating Temperature	0~70 C
Storage Temperature	-40~85 C
Size (W x D x H)	456 (W) × 485 (D) × 88 (H) mm

Appendix 3: Technical specifications of Silixa instrument

experts in distributed fibre optic sensing

ULTIMA™-S
High resolution Temperature Sensor

The ULTIMA-S has a continuous monitoring range of 5000 m per channel, a sampling resolution of 12.5cm and a minimum measurement time of 1 sec. The absolute temperature accuracy of the ULTIMA DTS is achieved by the automatic self-calibration of every measurement against an internal high-precision reference sensor. The Ultima-S has the best spatial resolution providing accurate measurements over the fibre length.

ULTIMA-S Specifications

Range
RANGE: 0-5 km

Channels
Option of either 4 or 8 channels

Operational Temperature
+5°C to +40°C

Power Requirements
Standby consumption: 108W at 5°C and 133W at 40°C.

Active consumption: 115W at 5°C and 143W at 40°C.

Measurement time
≥1 sec

Fibre type
Standard Graded Index (GI) 50/125µm multimode fibre

Dimensions
Width: 464.8mm

Height: 177.1mm

Depth: 467.4mm

Weight: 16.9kg

Silixa Ltd
Silixa House, Centennial Park
Centennial Avenue, Elstree
WD6 3SN, UK
www.silixa.com
t: +44 (0) 208 327 4210
f: +44 (0) 208 953 4062

VAT No.:GB 919 3229 14 Reg. No.: 6207412

ISOQAR 9032QM8001

Communication and Operating System

The ULTIMA-S includes a dual-core Intel Celeron processor and optoelectronic modules. It has an integrated hard drive of 80 GB, a serial port, an Ethernet port and 2 high speed USB ports. The Operating system is Windows based. Application software include ULTIMA Control and Acquisition and ULTIMA Data Viewer

Accessories included

2 x Pt100. The standard RTD probes have ±0.15°C absolute tolerance.

Certifications and Compliance

Safety: Class 1 Laser Product

- IEC 60825-1:Edition-2:2007
- EN 61010-1:2010

EMC

- EN61000-6-2:2005
- EN61000-6-4:2007
- EN61000-3-2:2006
- EN61000-3-3:2008

FCC

- CFR 47:2008 Part 15: B:2008

CE Mark

- 2006/95/EC (safety)
- 2004/108/EC (EMC)

Measurement Specifications

Temperature Resolution (ΔT)

The typical temperature resolution is shown in Figure 1. The Ultima-S 2km range, offers a temperature resolution of approximately 0.06°C at a distance of 2km over a period of 1 min for a 12.5cm sampling rate. The ULTIMA-S 5km range, offers a temperature resolution of approximately 0.4°C at a distance of 5km over a period of 1 min for a 12.5cm sampling rate. At longer measurement intervals the temperature resolution can be improved to 0.01°C at the near end and better than 0.03°C (5km variant) at the far end over longer measurement times. Figure 1 and Figure 2 show the temperature resolution of ULTIMA-S at 1s, 10s, 30s, 1min, 5min, 10min and 1h time averaged intervals over the 2km variant and 5km variant respectively.

Note that the ULTIMA-S can be configured by the user to achieve better temperature resolution at faster measurement times by increasing the spatial sampling. Spatial sampling options include 0.125, 0.25, 0.5, 1 and 2m.

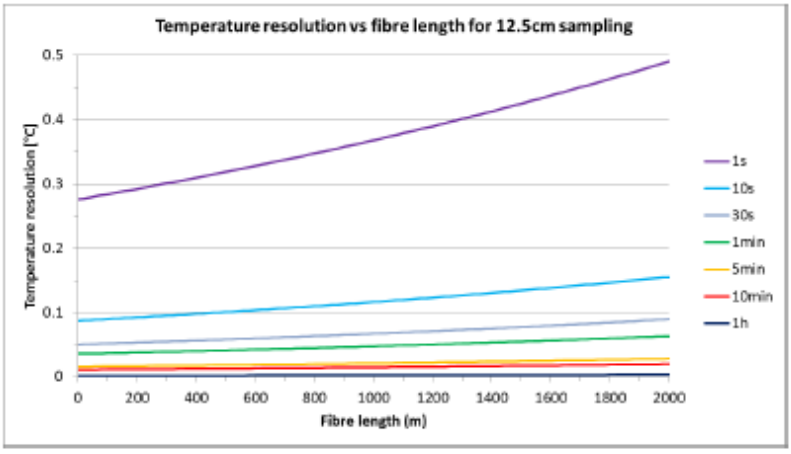

Figure 1: The temperature resolution (°C) is shown as a function of fibre length (m) at different averaging measurement times over the 2km variant.

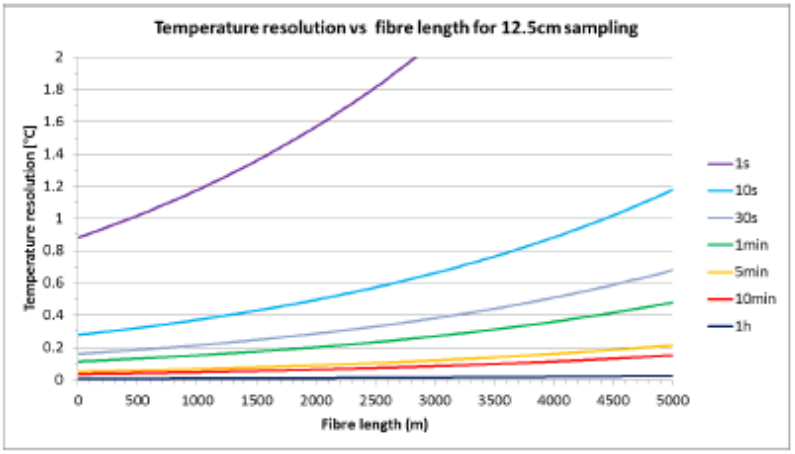

Figure 2: The temperature resolution (°C) is shown as a function of fibre length (m) at different averaging measurement times over the 5km variant.

Spatial Resolution (Δz)

The sampling resolution or sampling interval is the fibre length between consecutive temperature measurements. The spatial resolution defined as the length distance between a 10% and 90% temperature change of a given temperature step difference (typically $\Delta T \cong 30^{\circ}C$) is approximately 30cm. The spatial resolution is illustrated in Figure 3 over a step change of 30°C (measured at 29cm).

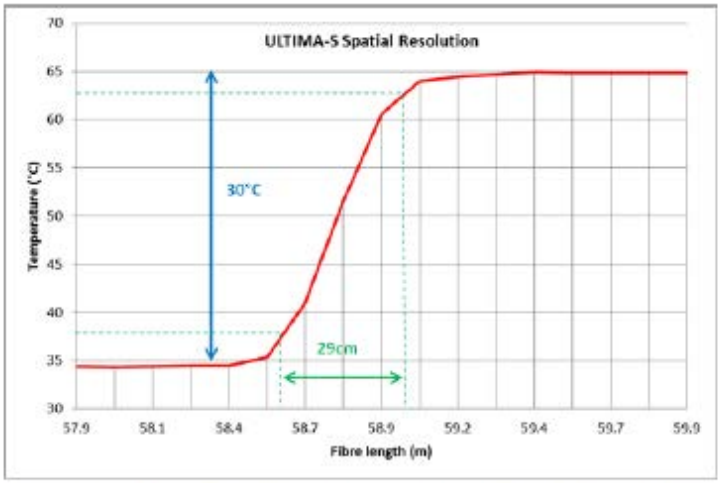

Figure 3: The spatial resolution of Ultima-S is shown as a function of fibre length (m) and temperature change (°C).